Spatial Learning and Localization in Animals: A Computational Model and its Implications for Mobile Robots

TR #97-20

Karthik Balakrishnan, Olivier Bousquet, and Vasant Honavar

September 24, 1997

Keywords:
spatial learning, spatial localization, place learning, place recognition, navigation, animal navigation, hippocampus, Kalman filter, probabilistic localization, dead-reckoning, spatial maps, topological maps, metric maps

ACM Computing Classification System Categories (1991):
I.2.2 [*Artificial Intelligence*] Automatic Programming — program modification, program synthesis;
I.2.6 [*Artificial Intelligence*] Learning — connectionism and neural nets, knowledge acquisition;
I.2.9 [*Artificial Intelligence*] Robotics;

Artificial Intelligence Research Group
Department of Computer Science
226 Atanasoff Hall
Iowa Sate University
Ames, Iowa. IA 50011-1040. USA
`http://www.cs.iastate.edu/~honavar/aigroup.html`

Spatial Learning and Localization in Animals: A Computational Model and its Implications for Mobile Robots

Karthik Balakrishnan*, Olivier Bousquet†, and Vasant Honavar‡
Artificial Intelligence Research Group
Department of Computer Science
Iowa State University, Ames, IA - 50011, USA
{balakris,bousquet,honavar}@cs.iastate.edu

Abstract

The ability to acquire a representation of the spatial environment and the ability to localize within it are essential for successful navigation in *a-priori* unknown environments. The hippocampal formation is believed to play a key role in spatial learning and navigation in animals. This paper briefly reviews the relevant neurobiological and cognitive data and their relation to computational models of spatial learning and localization used in mobile robots. It also describes a hippocampal model of spatial learning and navigation and analyzes it using Kalman filter based tools for information fusion from multiple uncertain sources. The resulting model allows a robot to learn a place-based, metric representation of space in *a-priori* unknown environments and to localize itself in a stochastically optimal manner. The paper also describes an algorithmic implementation of the model and results of several experiments that demonstrate its capabilities.

1 Introduction

The ability to successfully navigate in a wide range of natural environments is essential to the survival of animals. Mobile robots need to be equipped with similar capabilities in order to perform the tasks expected of them in natural or man-made environments. This requires them to be able to acquire and use adequate representations of their spatial environments. Animals offer compelling existence proofs of such capabilities that have evolved in nature (Anderson, 1983; Schone, 1984) and

*Karthik Balakrishnan was supported by an IBM graduate fellowship

†This research was performed during Olivier Bousquet's visit to Iowa State University. The visit was funded by Ecole Polytechnique, France.

‡This research was partially supported by the National Science Foundation through grant NSF IRI-9409580 to Vasant Honavar

challenge us to explore information processing mechanisms and computational architectures that can match their functionality, although they might be realized using different physical substrates and perhaps different design and performance constraints.

There is a large body of neuroanatomical, neurophysiological, and behavioral data on the possible role of different parts of the brain in general, and hippocampal formation in particular, in spatial learning and navigation (O'Keefe & Nadel, 1978; Churchland & Sejnowski, 1992). Computational models, although often simplified caricatures of their biological counterparts, provide an attractive approach to organizing, analyzing, abstracting, and exploring the implications of such data. In addition to suggesting new experiments designed to fill the gaps in our understanding of the systems being modeled, they are often very useful as sources of ideas for building artificial systems with comparable abilities. Against this background, a number of biologically inspired models of spatial learning, localization, and navigation have been proposed in the literature (Kuipers & Byun, 1991; Mataric, 1992; Kortenkamp, 1993; Kuipers *et al.*, 1993; Nehmzow, 1995; Recce & Harris, 1996).

On the other hand, those involved in the design of autonomous robots are necessarily faced with multiple design and performance constraints imposed by the available technology and the task environments. Attempts to address the attendant engineering challenges in the design of such systems have led to the development of a broad range of mathematical and computational tools. These include algorithms for the integration and use of noisy sensory data from multiple sensors (Ayache & Faugeras, 1987; Moutarlier & Chatila, 1989) and probabilistic localization (Smith *et al.*, 1990; Crowley, 1995). Use of such tools to analyze biologically inspired models can often yield new insights into the capabilities and limitations of the underlying information processing structures and processes (Levy, 1989).

The preceding discussion suggests that biologically inspired modeling efforts and the design of autonomous mobile robots can each benefit from the results and tools developed by the other. Against this background, this paper develops a biologically inspired model of spatial learning and localization for mobile robots. The relevant neuroanatomical, neurophysiological, and behavioral data on which the proposed model is based are summarized. The resulting model is compared with several other models that have been proposed in the literature. A Kalman filter based analysis of the model and its capabilities (in particular, the ability to function effectively in the presence of sensor and motion errors, and perceptual aliasing) is presented and the capabilities of the proposed

model are demonstrated using simulation experiments.

The remainder of the paper is organized as follows: Section 2 presents the requirements for goal-directed navigation by animals and autonomous mobile robots. These include learning, localization, and navigation. In section 3.2 we present neurobiological and cognitive aspects of spatial learning, representation, and navigation in animals, while section 5 briefly summarizes the different computational characterizations of hippocampal spatial learning. Our computational model is presented in section 6. The need for probabilistic localization is described in section 7 along with a summary of the Kalman filtering approach to robot localization. Section 8 develops a Kalman filtering framework for our computational model, while section 9 presents the details of our implementation. The results of our experimental simulations are presented in section 10. Other approaches related to the localization model developed in this paper are described in section 11. Finally section 12 provides a discussion including the contributions of this work to robot navigation. Some useful propositions are presented in the Appendix.

2 Spatial learning, localization, and navigation

Both animals and autonomous mobile robots need mechanisms to navigate purposefully in *a-priori* unknown (or partially known) environments. However, for such behaviors to be possible, they must be endowed with mechanisms to answer to the following questions (adapted from (Levitt & Lawton, 1990)):

1. Where am I? *(Localization)*
2. Where are other places relative to me? *(Map)*
3. Where is the goal? *(Goal identification)*
4. How do I get to the goal from here? *(Path planning)*
5. How do I acquire these things? *(Spatial learning)*

Although these questions appear straightforward, the answers are intricately intertwined, as might be expected. The first question is concerned with the identification or recognition of the current place, a problem commonly referred to as *localization* in robotics. Thus, places should be represented and remembered in terms of sensory features that allow the animal or robot to not only

distinguish between the different places in the environment but also reliably recognize places when visited. The second question deals with the representation of the spatial environment, which we refer to as a *map*. This map represents the relationship between places in the environment, and is a critical component of goal-directed navigation. Typically, *topological* and *metric* relationships are encoded in the maps as will be elaborated later. The third question is concerned with *goal identification* and is probably the most critical component of purposeful navigation. Indeed, if a goal is not explicitly known or is not identifiable based on the current information state of the animal or robot, goal-directed navigation is not possible. Goals may be specified in a number of ways, each suggesting a different navigation strategy based on the relationships encoded in the map. For instance, if goals are represented in terms of position information and the animal or robot knows its current position on the map, a direct trajectory to the goal can be computed by comparing the two positions. This is an example of metric navigation. The computation of the navigation trajectory is the answer to the fourth question, which is referred to as *path planning* in the robotics literature (see (Latombe, 1991; Hwang & Ahuja, 1992)). The navigation trajectory depends on the nature of information encoded in the map and also on the specification of the goal, and is additionally constrained by optimization concerns like determining the most efficient (shortest distance, least time, etc.) paths to the goal.

If the animal or robot has reliable answers to these questions, i.e., if it has a map of the environment, knows where it is on the map, knows the goal location on the map, and possesses the computational capability for determining a navigation trajectory, it can, indeed, navigate in a purposeful manner to arbitrary goals. If the environments are *a-priori* known and static, the maps can be pre-specified (and will not change), places can be well defined, and goals can be pre-determined, making purposeful navigation an outcome of *genetically programmed behaviors* in animals and *pre-wired control* in robots. However, the real-worlds occupied by animals and most robots are dynamic and at best *partially known*. In such cases, the animals and robots must possess mechanisms to *learn* and *adapt* to these environments they encounter. In the context of purposeful navigation, they must be able to identify and learn places, represent relationships between the places, and identify and learn goals. In short, they must have the capability of *spatial learning*.

In this paper we focus on only three of the above questions: spatial learning, representation, and localization. We consider how these processes are implemented in animals and develop a computational model of hippocampus-based spatial learning and localization. This model has

implications for spatial learning and localization in mobile robots, as we will clarify soon. But before we proceed, it would help to briefly consider the nature of spatial information representation in robots and animals.

3 Spatial learning and representation in animals and robots

If robots are to function successfully in natural environments, they should be equipped with mechanisms that are functionally similar to those used by animals in similar settings. This section explores the similarities between spatial representation and learning processes in animals and robots.

3.1 Representation of spatial information in robots

Contemporary robots usually represent spatial information in one of two ways: *metric* (*location-based*) or *relation-based* (Moutarlier & Chatila, 1989) (although some approaches have attempted to combine the merits of the two (Thrun, 1996; Levitt & Lawton, 1990; Kuipers & Byun, 1991; Kortenkamp, 1993)). In a metric representation of space, all the places (or object locations) are represented in the *same* coordinate frame. Thus, to compute the local relationship between two places, one has to perform some computation on their metric representations. However, since all the places are represented in the same coordinate frame, it is easy to compute direct, short-cut paths between two places by simply comparing their metric representations. On the other hand, relation-based approaches represent local relationships between places that are usually physically adjacent. Thus, the places are represented in different coordinate frames and significant computations might be needed to determine the global relationships between all the places. Further, to determine the direct trajectory between two arbitrary locations, a number of intervening transformations of local coordinate frames will be required.

An example of metric spatial representation in robots is the *occupancy grid* (Moravec & Elfes, 1985; Elfes, 1989) (or the more generalized *inference grid* (Elfes, 1992)), where a grid-like decomposition of the world is assumed. Each grid cell represents a portion of the environment, with adjacent grid cells representing adjacent physical locations in the environment. Cells in an occupancy grid are associated with a *probability of occupancy*, which is updated based on sensory input by using appropriate sensor models. Such grids can be easily learned and updated by the robot, often based just on sonar data. Since the grids provide a complete map of objects and

obstacles in the environment, a navigation trajectory can be computed by comparing the current robot position on the map with the location of the goal. However, since the grid represents the entire environment and not just the significant places, space is stored in an inefficient manner. Further, after each sensory measurement, the robot must update the occupancy probabilities of the entire grid, making it computationally expensive to maintain these maps. Also, increasing the grid-cell resolution (smaller grid cells) results in a quadratic (for 2D maps) increase in the number of cells required for the same environment, while decreasing the grid-resolution results in a loss of information and an increase in uncertainty (Elfes, 1992).

A popular example of relation-based spatial representation is the *topological map*. In these systems, space is represented in the form of a graph, with the nodes corresponding to *distinctive places* and the edges between nodes denoting the local relationship between the corresponding places (Kuipers, 1978; Brooks, 1985). Usually, distinctive places are defined based *sonar signatures* (Kuipers & Byun, 1991; Mataric, 1992; Kortenkamp, 1993), *image signatures* (Kortenkamp, 1993; Kortenkamp & Weymouth, 1994; Engelson, 1994), *panoramic views* (Tsuji & Li, 1993), *local occupancy grids* (Langley & Pfleger, 1995; Yamauchi & Langley, 1997), etc. The local relationships that are usually represented include the *directional* relationship between places (Nehmzow, 1995) or the directional relationship compounded with *distance* information (Kuipers & Byun, 1991). Some topological schemes also represent metric information pertaining to the distinctive place, which is useful if the place represents, say, a wall or a corridor (Mataric, 1992). Such relation-based approaches produce a compact world representation since they only represent distinctive places in the environment. Further, they are robust to global movement errors as they only represent local relationships between places (Brooks, 1985). These topological graphs can be learned through robot exploration. However, navigation to a goal requires a search through the graph to determine a *route* from the current robot location to the goal, which can be computationally expensive for large graphs.

These two representational approaches complement each other in useful ways, which has led to work in *multi-level representations* of spatial information (Levitt & Lawton, 1990; Kuipers & Byun, 1991; Kortenkamp, 1993; Thrun, 1996), some of which are discussed in section 11.

3.2 Spatial learning and representation in animals

For most animals, navigation is an essential component of its behavioral repertoire, which is needed to find food, mates, and avoid predators. This navigation is realized through several intricate mechanisms and processes (Anderson, 1983; Schone, 1984), which researchers are still trying to decipher. Based on data from neuroscientific and behavioral experiments with mammals, primarily rodents, O'Keefe and Nadel suggested that the *hippocampus* is a site for these spatial manipulations and that it learns a cognitive map representation of space (O'Keefe & Nadel, 1978). According to their thesis, the hippocampal formation allows the animal to learn and recognize places and build a metric representation of space by using dead-reckoning information (O'Keefe & Nadel, 1978).

Based on extensive behavioral experiments with rodents, researchers have concluded that space plays a dominant role in their behavior (Hebb, 1949). It also appears that rats give more importance to *remote sensory cues than to local ones*, possibly because remote cues are the *least-variable* objects in the environment (Hebb, 1949). Rats have also been found to successfully swim to a submerged platform in a milky pool of water thereby demonstrating an ability to compute trajectories to *hidden goal locations* (Morris, 1981). Other experiments have established that the rats appear to know how visual scenes are transformed by locomotion and are capable of computing approach trajectories using *inverse transformations* (Keith & McVety, 1988).

Experiments with gerbils have shed light on the nature of spatial representations, and it appears that these animals compute *vectors* to landmarks. Further, *independent* vectors are computed for each of the landmarks (Collett *et al.*, 1986). The researchers also found some evidence that suggested the grounding of internal spatial representations in a *locomotion-based metric system* (Collett *et al.*, 1986). This has led to the suggestion of a vector-based representation of space, according to which, a direct vector to a goal location can be computed by subtracting a vector from the goal location to a landmark from a vector to the same landmark from the current location (McNaughton *et al.*, 1995).

Experiments have also demonstrated that *stability* of landmarks is critical for spatial learning, i.e., even if a goal was constantly and reliably associated with a landmark, the rats failed to capture this relationship if the landmark (and the goal) were moved to different locations in each of the learning trials (Biegler & Morris, 1996). It appears that increasing the number of *stable spatial relationships* aids learning, rather than merely increasing the number or salience of the landmarks

(Biegler & Morris, 1996).

Thus, rodents appear to encode spatial information in the form of vectors to landmarks, with each of the landmarks being represented independently. Further, a locomotion-based metric system appears to be involved in the spatial representation, which critically depends on the stability of the landmarks.

Based on his studies with rats, Tolman suggested that spatial behavior is a result of *metric computations* that are made possible by spatial information stored in a metric form in *cognitive maps* (Tolman, 1948). However, Hull explained the experimental observations of Tolman in terms of the *habit-family hierarchy*, arguing that spatial behavior arises strictly through the association of specific *responses* with particular *stimuli* (Hull, 1934a; Hull, 1934b). O'Keefe and Nadel formalized the difference between these two theories of information representation, suggesting that animals (particularly rats) use at least two spatial representation and navigation systems: the *locale system* that corresponds to a cognitive map and represents spatial information in metric terms; and the *taxon system*, which is associated with stereotypic behaviors like route following (chapter 2, in (O'Keefe & Nadel, 1978)).

These two spatial information representation approaches in animals can be seen to parallel the metric and relation-based representation schemes used in contemporary robots described above. Thus at least at an abstract level, there appear to be unifying theories of spatial representation in animals and robots.

3.3 Role of path-integration in navigation

Path-integration, popularly known as dead-reckoning, refers to the process of updating an estimate of one's own position based on the knowledge of direction, speed, and time of self-motion (Gallistel, 1990). This usually involves integrating acceleration signals over time to obtain velocities, and the integration of velocity signals over time to obtain displacement vectors (Gallistel, 1990; Gallistel & Cramer, 1996).

There is substantial evidence for path-integration in animals (Wehner, 1992; Wehner & Srinivasan, 1981; Etienne, 1992; Gallistel, 1990). In their experiments, Mittelstaedt and Mittelstaedt found that gerbils could undertake circuitous search trajectories and then return on a direct bearing to the nest even in *complete darkness* (Mittelstaedt & Mittelstaedt, 1980; Mittelstaedt & Mittelstaedt, 1982). Based on experimental manipulations (like moving the nest to a different place),

they confirmed that the homing behavior was based on dead-reckoning. Additionally, they found gerbils capable of sensing and accurately correcting for *angular displacements* (e.g., turning of the entire arena), leading them to conclude that path-integration is based on *inertial* directional information from the vestibular system and *ideothetic* linear information involving proprioception and/or efference copy from the animal's self-generated motion (Mittelstaedt & Mittelstaedt, 1980; Mittelstaedt & Mittelstaedt, 1982).

Similar experiments have also been performed by other researchers on golden hamsters (Etienne, 1985; Etienne, 1992; Etienne *et al.*, 1996), which demonstrate that without frequent visual corroborations, path-integration systems rapidly accumulate errors. This has led to the suggestion that in the absence of visual information, path-integration appears to be useful only for short exploratory excursions from a known site (Etienne *et al.*, 1996). It has also been shown experimentally that in conflict situations between distant but familiar visual references and path-integration, the animals appear to give priority to stable visual references (Etienne *et al.*, 1990).

Thus, dead-reckoning behaviors are used by rodents to navigate. It also appears that animals have access to both sensory as well as path-integration input, and choose one over the other depending on their navigation context. Given the suggestion of locomotion-based metric representation of space, it is highly possible that this locomotion-based metric representation of space actually comes from path-integration.

Not surprisingly, dead-reckoning mechanisms have also been used in robot navigation (Kuipers & Byun, 1991; Kortenkamp, 1993; Yamauchi & Beer, 1996). As with animals, such behaviors have usually involved *homing*, where the robot returns to its *home-base* after executing its spatial task. Other uses of dead-reckoning have been in the building of metric spatial maps, with the dead-reckoning system providing a Cartesian coordinate representation of space. For instance, approaches for fusing *stochastic information* (e.g., Kalman filtering) have been used for robot localization and world modeling (Ayache & Faugeras, 1987; Moutarlier & Chatila, 1989; Crowley, 1995). In these approaches, dead-reckoning is used to provide estimates of robot position which are subsequently corrected based on observations. Recently, Yamauchi and Beer have defined a spatial representation scheme based on adaptive place networks, where Cartesian position estimates derived from dead-reckoning are used to represent regions of physical space (Yamauchi & Beer, 1996).

In the next section, we will show that animals represent space as a combination of sensory

and dead-reckoning information. Further, the information processing suggested for the animals is similar in principle to the stochastic information fusion approaches alluded to above.

4 Role of hippocampus in spatial learning

The evidence for implicating the *hippocampal formation* in spatial learning comes from two sources: *lesion studies* and *cellular recordings* of hippocampal cells. While lesion studies typically demonstrate the inability of hippocampal-lesioned animals to learn tasks of a spatial nature (e.g., mazes or object-place-matching tasks), cellular recordings show hippocampal involvement when the animal performs spatial tasks. We will briefly review the lesion data here and then present the anatomy and physiological properties of the hippocampal formation in more detail since they shed more light on the nature of spatial learning and representation.

In the neurobiological literature, the hippocampal formation and adjacent cortical regions of the medial temporal lobe have long been associated with spatial learning and memory (Churchland & Sejnowski, 1992), primarily through data that hippocampal lesions (or damage) produce severe learning deficits, including the ability to learn new stimuli, recognition memory, object-place task memory, etc. (Cohen & Eichenbaum, 1993; Churchland & Sejnowski, 1992). Hippocampal lesions have also been found to produce severe deficits in the ability of rodents to traverse complex mazes (cf. appendix of (O'Keefe & Nadel, 1978)). For instance, in the water-maze task (where rats have to swim to a submerged platform in a milky pool of water), rats with hippocampal damage are incapable of learning to navigate directly or efficiently to the hidden platform, although they appear perfectly capable of navigating accurately to a *visible* one (Morris *et al.*, 1982; Sutherland *et al.*, 1982).

4.1 Anatomy of the Hippocampal formation

The hippocampal formation is an association area of the brain that receives highly processed sensory information from the major associational areas of the cerebral cortex (Cohen & Eichenbaum, 1993) as shown in Figure 1. The inputs arrive at a major convergence area, collectively called the *parahippocampal cortical* area, which itself consists of the *perirhinal cortex*, the *parahippocampal cortex proper*, the *entorhinal cortex* (EC), and the *pre-* and *post-subiculum* (Squire *et al.*, 1989). The hippocampal formation is composed of the *dentate gyrus* (Dg), and areas *CA3* and *CA1* of

Ammon's horn, and for this reason, is often referred to as the *trisynaptic circuit*. The Dg receives input from the EC via the *perforant path*, and outputs to the CA3 via *mossy fibers*. These mossy fiber synapses with CA3 are rather strong, which has led researchers to suggest that they provide the *context* (O'Keefe, 1989) or *reference frame* (McNaughton *et al.*, 1996), possibly through *non-redundant* and *orthogonal* coding of the EC input (Rolls, 1996; Rolls, 1990).

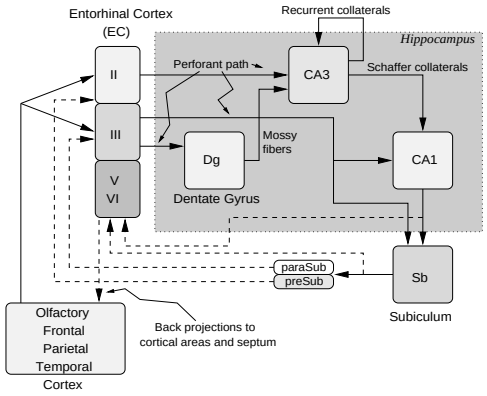

Figure 1: Anatomy of the hippocampal formation.

The CA3 region of the hippocampus primarily contains *pyramidal* (or complex-spike) cells along with inhibitory interneurons like *basket cells, chandelier cells, mossy cells,* etc. (Traub & Miles, 1991; Churchland & Sejnowski, 1992). These CA3 cells receive inputs from three different sources: from the EC through the perforant path, from Dg through mossy fibers, and finally recurrent inputs from other CA3 pyramidals. Some researchers have likened the structure of the recurrent collaterals to an autoassociative recurrent network suggesting that CA3 serves as a *pattern completion* device capable of recalling entire *scenes* from partially observed data (Marr, 1971; Rolls, 1990). However, others have ascribed a *hetero-association* role, suggesting that these collaterals *predict* future activations of the neurons based on the current activations (McNaughton, 1989; McNaughton & Nadel, 1989; Levy, 1989; Minai & Levy, 1993; Prepscius & Levy, 1994; Jensen & Lisman, 1996). Some experimental evidence for this view is provided by (Skaggs & McNaughton, 1996) and additional support comes from the observation of hippocampal activity *classical conditioning* tasks (Schmajuk, 1986; Schmajuk & DiCarlo, 1991; Churchland & Sejnowski, 1992).

The CA1 region of the hippocampus too consists of pyramidal cells and interneurons, however, unlike CA3 cells, CA1 cells do not project to other levels of CA1. The CA1 pyramidals receive

inputs from the EC via the perforant path and from the CA3 pyramidals through the *Schaffer collaterals*. Axons from the CA1 pyramidal neurons project via the alveus to the subiculum (Sb) and also to the EC. Sb also receives input from the EC and projects to the pre- and post-subiculum, the deep layers of the EC, and to the hypothalamus, septum, anterior thalamus and the cingulate cortex (Churchland & Sejnowski, 1992). Although it is not well studied yet, there is some evidence that the EC projects back to many of the cortical association areas from which it receives input and mediates information storage there (Churchland & Sejnowski, 1992). In addition, there is also some evidence that the hippocampal formation derives input and in turn outputs to the *fornix*. However, the nature of these projections is still unclear (Rolls, 1990). In the following section, we will describe some of the properties of hippocampal cells, which are critical to understanding some of the design choices made in our computational model.

4.2 Physiological properties of hippocampal cells

Cellular recordings from many regions of the brain, including the hippocampus, have revealed crucial properties of the underlying neuronal mechanisms. For instance, in their recordings from CA1 pyramidal cells of a rat hippocampus, O'Keefe and Dostrovsky found that the neurons were selectively active in particular regions of the environment of the moving rat (O'Keefe & Dostrovsky, 1971). O'Keefe later named them *place cells* and the corresponding regions where each is active, the *place field* (O'Keefe, 1976). Since then, cells with such location-specific firing have been found in almost every major region of the hippocampal system, including: the EC (Quirk *et al.*, 1992), the Dg (Jung & McNaughton, 1993), the hippocampus proper (O'Keefe & Dostrovsky, 1971; O'Keefe, 1976), the Sb (Barnes *et al.*, 1990; Sharp & Green, 1994), and the postsubiculum (Sharp, 1996).

In addition to place cells, *head-direction cells* have also been discovered. These cells appear to respond to particular directions of the animal's head, irrespective of its location in the environment. Each cell fires only when the animal's head faces one particular direction (over an approximately 90 degree range) in the horizontal place, and their relative directional tuning appears to be independent of the pitch and roll of the head. Further, the firing of these cells is dynamically alterable by a complex interaction between visual and angular motion signals. Importantly, in every case reported to date, any manipulation that alters the reference direction of one of these cells results in a corresponding alteration in the reference direction for the whole system. These cells were first discovered in the postsubicular area of the hippocampal formation (Ranck, 1984; Taube *et al.*,

1990a; Taube *et al.*, 1990b). Since then, such directional cells have also been discovered in the retrosplenial cortex (Chen *et al.*, 1994a; Chen *et al.*, 1994b), the anterior thalamus (Taube, 1995; Blair & Sharp, 1995), and the laterodorsal thalamus (Mizumori & Williams, 1993).

A number of experiments have been performed in order to determine the properties of the place and head-direction cells. It is now known that the spatial representation in the place cells is not *grid-like*, i.e., adjacent neurons are as likely to represent distant portions of the environment as close ones (O'Keefe, 1976; Muller *et al.*, 1987; O'Keefe & Speakman, 1987; O'Keefe, 1989; Wilson & McNaughton, 1993). Also, place cells are active in multiple places in the environment (O'Keefe & Speakman, 1987) and also in multiple environments (Kubie & Ranck, 1983; Muller *et al.*, 1987; Muller & Kubie, 1987). Further, places appear to be represented in the hippocampus using an *ensemble code*, i.e., a set of place cells appear to code for a place (Wilson & McNaughton, 1993).

Experiments have also revealed that when the animal is introduced into a familiar environment, place fields are initialized based on visual cues and landmarks (Muller & Kubie, 1987; Muller *et al.*, 1987; Sharp *et al.*, 1990). Once initialized, the place fields have been found to persist even if the visual cues are removed in the animal's presence (O'Keefe & Speakman, 1987), implying that place cell firing must also be maintained by a source other than visual stimulus. It has been found that place fields of CA1 cells are conserved in darkness, provided the animal is first allowed some exploration of the apparatus under illuminated conditions (McNaughton *et al.*, 1989; Quirk *et al.*, 1990). This has led to the hypothesis that place fields are maintained by ideothetic (self-motion) mechanisms, i.e., by the path-integration system.

Additionally, in familiar environments, visual inputs have been found to override vestibular inputs, i.e., when the entire environment is rotated, the place fields and the directional preference of head-direction cells, typically, but not always, rotate by an equivalent amount. In novel environments on the other hand, a rotation of the environment does not produce any noticeable change in the place fields or head-direction preferences (McNaughton *et al.*, 1995).

Similarly, head-direction cells have also been found to be responsive to visual inputs. It appears that rats develop stable, unique associations between visual stimuli and the cells of the path integration system, which allows them to automatically realign the path integration system when mismatches occur (Knierim *et al.*, 1995). However, if the rats were disoriented during training, they were unable to develop stable associations and consequently could not reorient their directional framework (Knierim *et al.*, 1995).

Finally, the role of the motor system in place and head-direction cell firing is shown by experiments involving motion restraints. When rats were wrapped in a towel thereby preventing movement of their limbs and transported *passively* through a familiar environment, hippocampal neuronal activity was seen to cease (Foster *et al.*, 1989). Normal hippocampal activity resumed when the restraint was removed. It was also noted that movement was not necessary for place cell activity to resume; it was sufficient that the animal could move if it wanted to (Foster *et al.*, 1989). A similar experiment has also shown the involvement of the motor system in the firing of head-direction cells in the thalamus (Knierim *et al.*, 1995). Since the path-integration system presumably receives input from the motor system (in the form of a motor efference copy or gating signals), these experiments further implicate path-integration in place and head-direction cell firing (McNaughton *et al.*, 1996).

In summary, place cells and head-direction cells respond to sensory as well as path-integration inputs. These cells are active in multiple environments and also active in multiple places in the same environment. The firing of these cells is conserved in darkness, provided the animal is first allowed to orient itself under lighted conditions. Finally, the firing of these cells is directly related to the motor system, and any restraint on active motion ceases cell firing.

5 Computational models of hippocampus-based navigation

Based on the data presented above and other results from behavioral experiments with humans and animals, a number of models have been proposed to explain the role of the hippocampal formation in animal navigation. These computational models can distinguished based on the type of navigation behavior performed by them, namely: *place-recognition triggered response* (or the *orientation-taxon hypothesis*), *topological navigation* (or the *guidance-taxon hypothesis*), and *metric navigation* (or the *locale hypothesis*). The strategies shown in parenthesis were suggested by (O'Keefe & Nadel, 1978), while the equivalent strategies outside the parenthesis were recently proposed by (Trullier *et al.*, 1997). These navigation behaviors are described below.

In place-recognition triggered response (PRTR), each place is associated with a navigation response that the animal performs when in that place. Usually the response is associated with a goal and the animal executes the response in order to approach the associated goal. Since goals are implicit in PRTR, so is the *motivation* (O'Keefe & Nadel, 1978). A number of hippocampal models

of spatial navigation fall into this category (Zipser, 1986; Burgess *et al.*, 1994; Brown & Sharp, 1995; Blum & Abbott, 1996; Burgess & O'Keefe, 1996). The primary advantage of PRTR systems is their *reactive* nature, i.e., the animal can produce a navigation response in *real-time* without the need for any lengthy computation since the response follows directly from the recognition of the place. Thus, these behaviors are *automatic* and *stereotypical* (O'Keefe & Nadel, 1978). However, these models encounter problems in environments with multiple goals. Apart from the model of (Burgess *et al.*, 1994; Burgess & O'Keefe, 1996), most other models are not capable of *latent learning*, i.e., simply learning a place map in the absence of an explicit goal. Also, these approaches usually break down when new obstacles appear in previously clear paths.

In topological navigation (TN), the animal learns places and associates adjacent places with the motion required to get from one place to the other. In such cases, goal-directed navigation reduces to determining a path from the current place to the place that houses the goal, using a procedure akin to a *graph search*. A number of models of spatial learning have been based on TN (Muller *et al.*, 1991; Kuipers & Byun, 1991; Mataric, 1992; Schmajuk & Thieme, 1992; Schmajuk & Blair, 1993; Bachelder & Waxman, 1994; Scholkopf & Mallot, 1995). Unlike PRTR, TN allows the animal to remember and follow different routes to the same goal and also remember routes to many different goals. Further, latent learning is also possible. However, goal-directed navigation in TN requires a search through the mental representation for a path to the goal, which can be computationally expensive. Further, the path is necessarily one that the animal has taken before. With such a scheme, the animal is usually incapable of devising and taking novel short-cut routes and detours, although with metric information recorded in the places (and on the links between them) the animal can perform the necessary computations to determine the metric relationship between the current place and the goal.

In metric navigation (MN), the animal learns places and labels them with position information in some metric framework computed by the animal. Thereupon, goal-directed navigation requires determining the current metric position of the animal, the position of the goal, and a computation to determine the approach vector from the current position to the goal (a vector subtraction). Surprisingly, there have been relatively few models of metric navigation (O'Keefe & Nadel, 1978; Prescott & Mayhew, 1992; Worden, 1992; Prescott, 1995; Wan *et al.*, 1994; Redish & Touretzky, 1996). even though the idea of a cognitive map (Tolman, 1948), and the suggestion that the hippocampus is the site for such a map (the locale system) have existed for a long while (O'Keefe

& Nadel, 1978). The primary advantage of MN approaches is the ability to compute a direct approach vector to the goal from the current place. In general, the computation will be more expensive than PRTR, but much less than the search effort required for TN. Although MN allows the animal to compute and follow novel short-cuts to goals, it runs into problems if the shortest-path to the goal either does not exist (e.g. between rooms in a building) or is blocked.

As can be observed, different aspects of neurophysiological, neuroanatomical, and behavioral data have led to different kinds of computational models. Further, each of these approaches have their own advantages and drawbacks. It is our belief that the hippocampus represents information of all three kinds: directional, topological, as well as metric. We believe that the navigating animal has access to these different kinds of information and it chooses an appropriate navigation strategy, or some combination of them, in ways suited to its current navigation context.

6 A computational model of hippocampal spatial learning

Based on the data summarized above and the suggestion that the hippocampus functions as a cognitive map (O'Keefe & Nadel, 1978), we have developed a computational model of hippocampal spatial learning that represents space in a metric framework (Balakrishnan & Honavar, 1997a; Balakrishnan & Honavar, 1997b; Bousquet *et al.*, 1997). The animal's environment is compactly represented as *distinct places*, with the center of each place also being labeled with metric information derived from dead-reckoning. If the spatial locations of the goals are also represented (in the same coordinate system as dead-reckoning), the animal can easily navigate to the goal by computing the vector-difference between its current metric position and the goal location.

In our model, sensory input-driven place codes are produced in the CA3 layer, which are associated with dead-reckoning based position information (possibly from the caudate nucleus (Potegal, 1972; Abraham *et al.*, 1983)), in the CA1 layer. Since many places in the animal's environment can produce the same sensory inputs (known as *perceptual aliasing* in robotics), the place codes of CA3 will not correspond to unique places. We suggest that dead-reckoning information is used by the animal to resolve such conflicts in the CA1 layer. Although this idea is intuitively obvious, to the best of our knowledge, no one has ascribed such a role to CA1 cell firing. The overall schematic of our computational model is shown in Figure 2 and its functioning can be briefly summarized as follows.

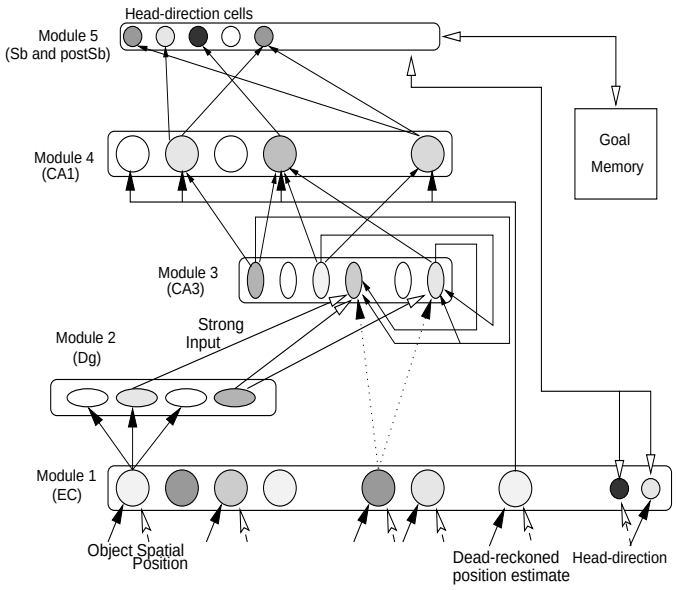

Figure 2: Computational model of the hippocampus.

As the animal explores its environment, new sensory-input driven EC units are recruited. These units respond to specific kinds of landmarks located at particular positions relative to the animal. Places are defined by concurrently active EC units and CA3 place cells are recruited to represent these places. These sensory input-driven CA3 place cells are then associated with position estimate from the path-integration system through Hebbian-like learning in the CA1 layer. Thus, the CA1 unit firing is dependent on sensory inputs from CA3 as well as path-integration. As mentioned earlier, the CA1 cells in our model not only create a metric representation of space but also disambiguate between perceptually similar places. Our model also assumes that the CA3 recurrents use motion information derived from a motor efference copy or ideothetic means to associate places with animal motion required to get from one place to the other. However, this is not implemented in our current model. It is also possible to associate head-direction information with the place code of CA1 in the postsubiculum. Again, this is not implemented in the model described in this paper.

Incoming sensory inputs activate a place code in the CA3 layer through a competitive activation procedure. This CA3 code is used along with the dead-reckoning input to determine the unique CA1 place code that corresponds to the current place. The hippocampal system performs spatial localization by *matching* the *predicted* position of the animal (from the dead-reckoning system) with the *observed* position of the place field center (dead-reckoning estimate stored with the activated

CA1 place code). Based on this match, the dead-reckoning estimate as well as the place field center are updated as shown in Figure 3.

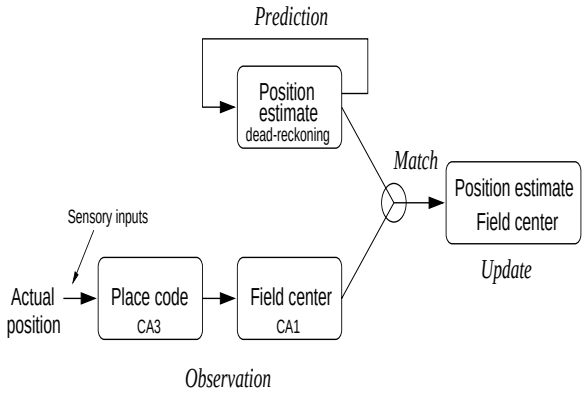

Figure 3: A schematic of hippocampal localization.

In a familiar environment, the animal places high confidence in its dead-reckoning based position estimate. Under these circumstances, even if some landmarks are removed, the high confidence in path-integration overrides the changed sensory activation, allowing the animal to still correctly identify the place. We believe that changes in the EC-CA3 as well as EC-Dg synapses soon align the place code with the new sensory input. Upon reintroduction into a familiar environment, the animal initially distrusts its path-integration estimate and also possibly its head-direction estimate. Visual (or sensory) inputs activate place codes which can then be used to initialize (or correct) the animal's position (from CA1) and head-direction (from post-Sb) estimates.

In our model, place fields are quickly formed through exploration. The CA1 place cells are driven both by sensory as well as path-integration inputs, thus they can be manipulated by changes in the landmark configuration and yet continue to fire in darkness. The CA3 fields, on the other hand, do not have direct path-integration input. However, once visually initialized, they will continue to fire in darkness owing to the recurrent collaterals, which provide place predictions based on motion. In darkness, without the appropriate updates of Figure 3, the position estimates accumulate drifts and the place cell firing in CA3 and CA1 becomes erratic.

Although the role of dead-reckoning in place cell firing was suggested by O'Keefe and Nadel, they did not provide a concrete computational realization of the hypothesized mechanisms (O'Keefe & Nadel, 1978). Our model assumes that dead-reckoning information is made available to the hippocampus, which performs spatial learning and localization to maintain reliable dead-reckoning

estimates. This is in contrast to the thesis of (McNaughton *et al.*, 1996) who suggest that the hippocampus *performs* dead-reckoning (McNaughton *et al.*, 1996). Our model is closely related to the theory proposed by Touretzky and colleagues (Wan *et al.*, 1994; Redish & Touretzky, 1996). However the two models differ in the manner in which the sensory inputs are made available to the place cells. In their model, place cells are tuned to two landmarks, a retinal angle, and dead-reckoning coordinates. In contrast, we model place cells in the EC layer as *landmark recognizers* that respond to specific landmarks at particular vector positions in relation to the animal. This EC activation forms the basis of place cell firing in the CA3 layer. The CA1 input is derived from these CA3 activations and dead-reckoning estimates. Our model also suggests specific roles for the different hippocampal regions, which are motivated by experimental data in many cases and serve as predictions in others (Balakrishnan & Honavar, 1997a). Another important difference between the models is our suggestion that the CA1 uses dead-reckoning information to overcome perceptual aliasing problems. Finally, our model treats the hippocampal inputs as uncertain quantities (sensory/recognition uncertainty and path-integration errors), and performs probabilistic information fusion and updates.

7 Probabilistic localization

In our model of the hippocampus as a spatial localization system, we have suggested that the hippocampus integrates information from two streams: the sensory inputs and the path-integration system. It should be noted that information provided by both these streams is uncertain. Sensory systems of animals accommodate considerable errors (for e.g., in the estimation of distance and direction to visible objects, recognition of objects, etc.). Path-integration is also prone to estimation errors and drifts, and the very fact that place cell (and head-direction cell) firing drifts in darkness is suggestive of errors in path-integration. Thus, in order for the hippocampus to perform robust spatial localization using these uncertain information sources, it must necessarily be capable of *probabilistic localization* (localizing by using probabilistic techniques to handle the uncertainties in appropriate ways). Although several hippocampal models of spatial learning have been proposed, some of them closely related to our own, none of the models are capable of explicitly handling such uncertain data. Thus, we need a probabilistic framework for characterizing hippocampal information integration.

As with animals, mobile robots too have to deal with uncertainties in sensing and action. This has led to many probabilistic localization approaches for mobile robots. One such localization tool is the *Kalman filter* (Kalman, 1960; Gelb, 1974; Crowley, 1995) (or some extension or generalization of it), which allows the robot to build and maintain a *stochastic spatial map* (Smith *et al.*, 1990), propagate sensory and motion uncertainties, and localize in *optimal* ways (Ayache & Faugeras, 1987). This probabilistic localization approach is discussed below.

7.1 Robot localization using a Kalman Filter

The Kalman filter technique for robot localization typically maintains a stochastic map of the robot's environment at each discrete time-step k (called the state vector $\mathbf{x}_k$), which includes an estimate of the robot's current position and possibly the estimated positions of other landmarks in the robot's environment. It is assumed that the *system model*, denoting the evolution of the state based on robot motion, is specified:

$$\mathbf{x}_k = \mathbf{\Phi}_{k-1}\mathbf{x}_{k-1} + \mathbf{u}_{k-1} + \mathbf{v}_{k-1} \tag{1}$$

where $\mathbf{u}_{k-1}$ is the *movement command* and $\mathbf{v}_{k-1}$ is the motion error with variance matrix $\mathbf{Q}_{k-1}$. Also, a *measurement model* is assumed to be given, which denotes the measurements or observations the robot would make when in a given state $\mathbf{x}_k$:

$$\mathbf{z}_k = \mathbf{H}_k\mathbf{x}_k + \mathbf{w}_k \tag{2}$$

where $\mathbf{w}_k$ is the measurement noise with variance matrix $\mathbf{R}_k$.

Given these two models, the Kalman filter stores and updates an *estimate* of the current state $\hat{\mathbf{x}}_k$ and its associated covariance matrix $\mathbf{P}_k = E\{(\mathbf{x}_k - \hat{\mathbf{x}}_k)(\mathbf{x}_k - \hat{\mathbf{x}}_k)^T\}$, by making *predictions* and combining them with *observations*. Suppose the current state estimate is $\hat{\mathbf{x}}^+_{k-1}$ with the covariance matrix $\mathbf{P}^+_{k-1}$. Based on robot motion, the Kalman filter predicts the new state of the system $\hat{\mathbf{x}}^-_k$, using equation 1 with an estimate of $\mathbf{0}$ for the motion error $\mathbf{v}_{k-1}$. The corresponding covariance matrix is updated to $\mathbf{P}^-_k = \Phi_{k-1}\mathbf{P}^+_{k-1}\Phi^T_{k-1} + \mathbf{Q}_{k-1}$. Based on this state prediction and using the sensor model $\mathbf{H}$, the system predicts the measurement $\mathbf{H}_k\hat{\mathbf{x}}^-_k$ using equation 2. This is the sensory input the robot is predicted to observe at its predicted position. Based on actual measurement $\mathbf{z}_k$, the Kalman filter then allows the state estimate and covariance matrix to be updated as follows

(refer to (Gelb, 1974) for details of the derivation):

$$\hat{\mathbf{x}}_k^+ = \hat{\mathbf{x}}_k^- + \mathbf{K}_k(\mathbf{z}_k - \mathbf{H}_k\hat{\mathbf{x}}_k^-) \quad (3)$$

$$\mathbf{P}_k^+ = (\mathbf{I} - \mathbf{K}_k\mathbf{H}_k)\mathbf{P}_k^- \quad (4)$$

where $\mathbf{K}_k = \mathbf{P}_k^-\mathbf{H}_k^T(\mathbf{H}_k\mathbf{P}_k^-\mathbf{H}_k^T + \mathbf{R}_k)^{-1}$ is the *Kalman gain* and $\mathbf{z}_k - \mathbf{H}_k\hat{\mathbf{x}}_k^-$ is called the *innovation*. This Kalman filter formulation is recursive and the process is repeated as the robot moves. This process can be described by the schematic shown in Figure 4.

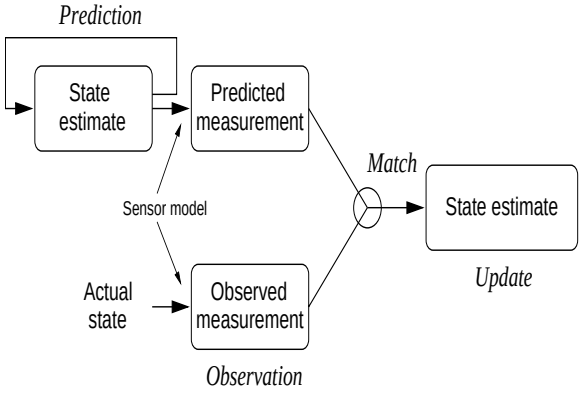

Figure 4: A schematic of Kalman filtering.

It can be shown that the Kalman filter update expressions shown above correspond to an estimation process that is *optimal* (minimum variance, maximum likelihood, etc.), provided the system and measurement models are linear, and $\mathbf{v}$ and $\mathbf{w}$ are assumed to be uncorrelated, zero-mean, white Gaussian noise (Maybeck, 1990). (Note: uncorrelated means $E(\mathbf{w}_i\mathbf{v}_j) = 0$ for all i, j; zero-mean implies $E(\mathbf{v}_i) = 0$ and $E(\mathbf{w}_j) = 0$; and whiteness refers to $E(\mathbf{w}_i\mathbf{w}_j^T) = \delta_{ij}\mathbf{R}_i$ and $E(\mathbf{v}_i\mathbf{v}_j^T) = \delta_{ij}\mathbf{Q}_i$, where δ_{ij} is the *Kronecker delta function* ($\delta_{ij} = 1$ iff i=j, and 0 otherwise) and $\mathbf{Q}_i$ is the covariance matrix of the random noise $\mathbf{v}_i$ and $\mathbf{R}_i$ is the covariance matrix of the random noise $\mathbf{w}_i$.)

8 Hippocampal Kalman filtering

As can be observed from Figures 3 and 4, our computational model of hippocampal function and Kalman filter both share the same *predict-observe-match-update* principle. Further, Kalman filter provides a framework for performing stochastically optimal updates even in the presence of prediction and observation errors. Since one of our goals is to develop a framework for uncertain

information fusion in our hippocampal model, it is interesting to explore whether hippocampal function could be described in terms of Kalman filtering theory. If so, one can apply Kalman filtering theory to characterize information processing in the hippocampus and use it in practical computational realizations. In what follows, we develop a Kalman filtering framework for our hippocampal localization model.

8.1 State vector representation

In robot localization, the state vector usually contains the position of the robot and the positions of landmarks in the robot's environment. Since spatial localization in the hippocampus appears to be based on *place recognition*, we have to use a state vector that contains the locations of these places. In our computational model, places are characterized by their centers which are represented in terms of dead-reckoning estimates. Thus, we use a state vector that is composed of the estimated *centers* of places encountered by the animal and represented in the CA1 layer. It should be borne in mind that this notion of center is probabilistic, i.e., it is the expected position of the animal given that the corresponding place has been recognized. Mathematically, $x_i = E(x_0|i)$, where x_0 is the position of the animal and x_i is the center of place i. To keep the discussion simple we will henceforth assume that place codes in CA3 and CA1 are represented by single units, although in reality ensembles of units are known to code for place (Wilson & McNaughton, 1993). Thus, the state vector is given by:

$$\mathbf{x}_k = [x_{0,k}, x_1, \ldots, x_n]^T \tag{5}$$

where $x_{0,k}$ denotes the position of the animal, x_i denotes the center of place field i, and n is the number of places that have been visited by the animal. In this paper we assume that these positions (animal position and place field centers) are specified in 2D Cartesian coordinates, i.e., $x_i = (x_{i_x}, x_{i_y})$. We do not consider the *orientation* of the animal (or a place) for two reasons. Firstly, this simplifies the model and makes the computations easier to characterize. Secondly, our computational model currently does not have a mechanism for updating head-direction estimates.

The covariance matrix associated with this state vector, denoted by $\mathbf{P}_k$, is given by:

$$\mathbf{P}_k = \begin{pmatrix} \mathbf{C}_{00} & \mathbf{C}_{01} & .. & \mathbf{C}_{0n} \\ \mathbf{C}_{10} & \mathbf{C}_{11} & .. & \mathbf{C}_{1n} \\ . & . & . & . \\ . & . & . & . \\ \mathbf{C}_{n0} & \mathbf{C}_{n1} & .. & \mathbf{C}_{nn} \end{pmatrix}$$

where

$$\mathbf{C}_{ij} = \begin{pmatrix} C_{i_x j_x} & C_{i_y j_x} \\ C_{j_x i_x} & C_{j_y i_y} \end{pmatrix}$$

denotes the covariance between the 2D Cartesian representations of the state elements $x_i = (x_{i_x}, x_{i_y})$ and $x_j = (x_{j_x}, x_{j_y})$.

When a new place is visited, the state vector is augmented by the center of this new place and the state estimate and its covariance matrix are modified accordingly.

8.2 The system model

The system model in Kalman filtering describes the change in the state vector with the robot's motion. Importantly, given the robot motion, it allows one to predict the new state vector. In our hippocampal model, dead-reckoning provides a *prediction* of the animal's position based on its motion. However, dead-reckoning is error prone, leading to the following modified system models:

$$\begin{array}{lll} \mathbf{x}_k &= \mathbf{\Phi}_{k-1}\mathbf{x}_{k-1} + \mathbf{u}_{k-1} & \text{Animal motion} \\ \hat{\mathbf{x}}_k^- &= \mathbf{\Phi}_{k-1}\hat{\mathbf{x}}_{k-1}^+ + \mathbf{u}_{k-1} + \mathbf{v}_{k-1} & \text{Dead-reckoning estimate} \end{array}$$

Here, $\mathbf{u}_{k-1}$ includes the intended motion of the animal and possibly the motion errors. The dead-reckoning system produces a position estimate based on the animal's motion $\mathbf{u}_{k-1}$ and a zero-mean white noise $\mathbf{v}_{k-1}$ (with covariance matrix $\mathbf{Q}_{k-1}$) that characterizes the dead-reckoning model. This is different from the formulation in regular Kalman filtering and requires that we know the dead-reckoning system model (i.e., its covariance matrix).

Since the place field centers do not change with animal motion and only the position estimate of the animal changes, we can make the following simplifications $\mathbf{u}_k = [u_k, 0, \ldots, 0]^T$ and $\mathbf{v}_k = [v_k, 0, \ldots, 0]^T$. Further, if we assume that the animal only translates in the direction it is facing or turns in the same place, we can take $\mathbf{\Phi}_k = \mathbf{I}$, leading to the following *linear* system models for animal motion and dead-reckoning:

$$\begin{array}{lll} x_{0,k} &= x_{0,k-1} + u_{k-1} & \text{Animal motion} \\ \hat{x}_{0,k}^- &= \hat{x}_{0,k-1}^+ + u_{k-1} + v_{k-1} & \text{Dead-reckoning estimate} \end{array}$$

8.3 The measurement model

For Kalman filtering, we also need to specify the measurement model that allows one to predict measurements and compare it with observed ones. In our hippocampal model, sensory inputs activate (or permit recognition of) the place i_k where the animal is currently located. Given this

observation of a place, we might be tempted to treat $\hat{x}_{i_k}$ (the center of the recognized place) as the observation and the dead-reckoning generated $\hat{x}_{0,k}$ as the prediction, and apply Kalman filtering. However, this cannot be done because the observation and prediction are correlated (since $\hat{x}_{i_k}$ is some previous value of $\hat{x}_{0,k}$). Other alternatives must be explored. One possibility is to choose the measurement model: $z_k = x_{0,k} - x_{i_k} + w_k$ which represents a vector from the position of the animal ($x_{0,k}$) to the center (x_{i_k}) of place i_k where the animal finds itself at time step k. Although we can predict the measurement based on the estimated values of $\hat{x}_{0,k}$ and $\hat{x}_{i_k}$, we cannot observe z_k since we do not know the true centers of the places or the exact position of the animal.

This problem can be circumvented by specifying a measurement function that always observes $z_k = x_{0,k} - x_{i_k} + w_k = 0$, which is equivalent to saying that the measurement model always observes the animal at the center of a place field. This measurement function constrains the form of the random error to $w_k = x_{i_k} - x_{0,k}$ (proposition 3). It can be shown that v_k still has zero-mean (proposition 4), provided the animal navigates randomly between place fields or moves from one place field center to another. However, it turns out that it is *autocorrelated* and hence is not a white sequence (proposition 5). This autocorrelation is difficult to measure, and though we could use extended state vectors to estimate this correlation, leading to augmented Kalman filtering (pp 212, (Jazwinski, 1970)), we simply choose to ignore it. The justification for this is provided by the navigation behavior of the animal. If the animal moves to random positions in the place fields this autocorrelation will be zero, since the current displacement of the animal from the center of the current place field will not be related to its displacement in the previous step (due to the intervening random motion). On the other hand, if the animal moves purposefully from one place field center to the other, the correlation will be very small since the magnitude of the errors (w_k) can be expected to be small. Since it is reasonable to assume that the animal moves randomly during exploration and subsequently from one place field center to the next, we can ignore this autocorrelation term in our computations. Indeed, in our simulations we found this autocorrelation to be negligible.

Thus, if the sensory input at a given place corresponds to a place i_k, we use $\mathbf{H}_k\mathbf{x}_k = x_{0,k} - x_{i_k}$ and $\mathbf{w}_k = w_k$ to obtain the measurement model and predicted measurements as:

$$\begin{aligned} z_k &= x_{0,k} - x_{i_k} + w_k = 0 \quad \text{Observed measurement} \\ \hat{z}_k &= \hat{x}^-_{0,k} - \hat{x}^-_{i_k} \qquad\qquad\quad \text{Predicted measurement} \end{aligned}$$

8.4 Update expressions

Using the state vector representation and the system and measurement models described above, it can be shown that a minimum-variance derivation akin to Kalman filtering leads to the following update rules.

Based on the animal's motion, the dead-reckoning system generates a position prediction:

$$\hat{x}^-_{0,k} = \hat{x}^+_{0,k-1} + u_{k-1} + v_{k-1} \tag{6}$$

The elements of the covariance matrix associated with the state are also updated as follows:

$$\begin{aligned} C^-_{00} &= C^+_{00} + \mathbf{Q}_{k-1} \\ C^-_{ij} &= C^+_{ij} \qquad\qquad \forall \text{i,j not both 0} \end{aligned}$$

Based on its sensory inputs, suppose the animal identifies the place as i_k. Kalman filter update rules shown in section 7.1 can then be shown to reduce to the following expressions, leading to the update of the dead-reckoning position estimate and its variance as follows:

$$\hat{x}^-_{0,k} = \hat{x}^-_{0,k} - (C^-_{00} - C^-_{0i_k})(C^-_{00} - 2C^-_{0i_k} + C^-_{i_k i_k} + \mathbf{R}_k)^{-1}(\hat{x}^-_{0,k} - \hat{x}^-_{i_k}) \tag{7}$$

$$C^+_{00} = C^-_{00} - (C^-_{00} - C^-_{0i_k})(C^-_{00} - 2C^-_{0i_k} + C^-_{i_k i_k} + \mathbf{R}_k)^{-1}(C^-_{00} - C^-_{0i_k}) \tag{8}$$

Similarly, the place field centers and their variances are updated using:

$$\hat{x}^+_m = \hat{x}^-_m - (C^-_{m0} - C^-_{mi_k})(C^-_{00} - 2C^-_{0i_k} + C^-_{i_k i_k} + \mathbf{R}_k)^{-1}(\hat{x}^-_{0,k} - \hat{x}^-_{i_k}) \tag{9}$$

$$C^+_{mn} = C^-_{mn} - (C^-_{m0} - C^-_{mi_k})(C^-_{00} - 2C^-_{0i_k} + C^-_{i_k i_k} + \mathbf{R}_k)^{-1}(C^-_{n0} - C^-_{ni_k}) \tag{10}$$

8.5 Distinguishing perceptually similar places

Often, different locations in the environment produce the same sensory input (perceptual aliasing) and we need mechanisms to handle such cases. In our model, we suggested that these aliasing problems in CA3 are resolved by CA1 using dead-reckoning information. It appears that we can use another tool from robotics to elegantly make such distinctions, namely, the *Mahalanobis distance* (Ayache & Faugeras, 1987). Mahalanobis distance is a metric that computes the difference between predicted and observed values and normalizes them by their covariance. This distance measure has a χ^2 distribution with q degrees of freedom where q is the rank of the covariance matrix (Ayache & Faugeras, 1987; Crowley, 1995). Since the errors in our system are assumed to be Gaussian and the system equations are linear, we can use the Mahalanobis test to perform

matches. This is used as follows. Suppose the animal is currently at a position $x_{0,k}$ and the sensory inputs activate a CA3 place code. Further, let us assume that this place code is associated with a CA1 code i_k with estimated place field center $\hat{x}_{i_k}$. Given the current estimate of the animal's position $\hat{x}_{0,k}$, we perform the following test:

$$(\hat{x}_{0,k} - \hat{x}_{i_k})^T (C_{ii} + C_{00} - 2C_{0i} + \mathbf{R}_k)^{-1} (\hat{x}_{0,k} - \hat{x}_{i_k}) < \epsilon \tag{11}$$

where $(C_{ii} + C_{00} - 2C_{0i} + \mathbf{R}_k)$ is the covariance matrix (proposition 6) and ϵ is a threshold that is chosen appropriately (proposition 7).

If condition 11 holds, then we assert that the place has indeed been visited before and CA1 unit i_k represents the place. However, if this test fails, it implies that the animal is now at a *new* place that perceptually resembles some other place visited earlier. In this case, we recruit a new place cell in the CA1 layer and include its parameters in the state vector. Thus, our system creates multiple units in the CA1 layer that repond to the same sensory input in the CA3 layer, but are tuned to different centers that correspond to the peaks of the multimodal distribution $P(x|s)$ (where s is some sensory input).

9 Implementation

The localization model described above was implemented on a simulated robot. In this section we discuss the implementation of the proposed computational model, including the algorithms used for place learning and localization.

9.1 Sensory inputs

We assume that our robot is endowed with a set of sensors that provide information pertaining to landmarks in the environment along with their positions relative to the robot. In our simulation, these sensors are *virtual* and can be implemented on real robots through a variety of physical devices. Although landmark recognition is error-prone in general, we assume that the landmarks are recognized accurately in our simulation. However, the range information is imprecise in our simulation, and the actual position of the landmark (x_l, y_l) is considered to be corrupted by zero-mean, white Gaussian noise with variance σ_S^2.

9.2 Representation of EC cells

In our model, EC place cells function as *spatial filters*, responding to particular kinds of landmarks at specific positions relative to the animal. We use an EC representation where each cell stores some internal description of a landmark as well as the Cartesian position of the landmark with respect to the animal (the EC field center). This landmark position is *allocentric*, i.e., it is not dependent on the direction in which the robot is facing. This stored information is matched against incoming sensory information. While the landmark identity is matched directly, the x and y coordinates of the landmark are matched with the EC field center using a *two-dimensional Gaussian function* with variance σ_L^2. The algorithm for determining EC layer firing is given below:

1. Set the EC output to zero, i.e., $\forall$ EC cells i, ECOutput(i)=0.

2. For each landmark L that is currently sensed at a position (x_L, y_L) relative to the robot do:

   (a) Determine the activation, ECAct(i), of each EC cell i by the matching procedure described above.

   (b) If none of the cells produce an activation greater than a threshold (, $_{EC}$), recruit a new EC cell j. Set its parameters to the identity of landmark L and to its position x_L and y_L. Set ECOutput(j)=1.0. Exit.

   (c) Else, determine each cell i that fires above the threshold (, $_{EC}$). Set ECOutput(i) = max (ECOutput(i), ECAct(i)).

Thus, EC units are created when landmarks are observed in positions not seen before. Also, each EC cell responds to landmarks in a region specified by its center. The radius of this region is computed in proposition 1.

9.3 Place codes in CA3

Our implementation currently ignores the Dg layer. Further, for simplicity, the place codes in CA3 are assumed to be given by single units rather than ensembles of them (although the theory can be easily extended to handle ensemble coding of space). Each CA3 cell is connected to EC cells that are active in a given place. The algorithm used to set up CA3 cells is given below:

1. Determine the output of the EC layer.

2. Compute the output of each CA3 cell i as: CA3Output(i) = $\sum_{\forall \text{EC j}} ECOutput(j) \times w_{ij}$, where w_{ij} is the weight between EC unit j and CA3 unit i.

3. If none of the CA3 units produce an activation greater than , $_{CA3}$, recruit a new CA3 unit i and connect it to each EC unit j with a weight given by: $w_{ij} = \frac{ECOutput(j)}{\sum_{\forall \text{EC k}} ECOutput(k)}$. Exit.

4. Else, determine the CA3 unit k that has the highest activation of all and declare it the *winner*.

Thus, a place is said to be recognized if the winning CA3 place unit produces an activation greater than the threshold , $_{CA3}$. If all the CA3 units have an activation below the threshold, the robot is said to be in a new place and a new CA3 unit is created.

9.4 Unique place recognition in CA1

Each CA1 unit in our model is connected to a CA3 unit and to path-integration information derived from the EC. Note that for the sake of simplicity, we again use single units to denote the place cells of CA1. The algorithm for determining CA1 activation is as follows:

1. If a new CA3 unit was created, recruit a new CA1 unit and connect it to the newly created CA3 unit with a weight of 1. Also, store the x and y coordinates of the current position estimate from dead-reckoning with the new CA1 unit. Exit.

2. Else, for each CA1 unit i connected to the winning CA3 unit, compute the Mahalanobis distance between the current position estimate from dead-reckoning and the position estimate stored at unit i.

3. Determine the winner, i.e., the CA1 unit j producing the least Mahalanobis distance.

4. If this distance is less than , $_{CA1}$ update the position estimate as well as the stored place field centers using the Kalman filter update rules. Exit.

5. Else, create a new CA1 unit and connect it to the winning unit in the CA3 layer with a weight of 1. Store the current position estimates with the new CA1 unit.

As shown above, CA1 units are created when the animal visits a new place or if the Mahalanobis distance of the best matching place is greater than the threshold , $_{CA1}$.

10 Experiments

This section describes the particulars of the simulation environment used in our experiments and also the values of the different parameters that were used. It also describes the experiments that were performed and presents the results.

10.1 Experimental setup

In our experiments, the simulated robot is assumed to operate in a room containing four identical landmarks, as shown in Figure 5. Although the room is not delimited by walls, we only show a 20×20 region of the room. The landmarks are placed as shown in Figure 5. The robot starts at position A with dead-reckoning estimates set to $(0, 0)$ and attempts to follow a circular clockwise trajectory. With each movement, the robot updates its dead-reckoning estimate accordingly. Since our simulated robot does not have any dead-reckoning apparatus, we model dead-reckoning errors as zero-mean Gaussians with standard deviation $\sigma_M = 0.1$. The robot is assumed to have a faithful compass, and hence knows the allocentric directions of the sensed landmarks. However, the sensed range of landmarks is assumed to be corrupted by a zero-mean Gaussian noise with a standard deviation of $\sigma_S = 0.01$ per unit distance. This error value of 1% per unit distance is compatible with contemporary sonar-based distance ranging (Everett, 1995).

As explained earlier, the sensed landmark information is provided as input to the EC layer. In our simulations, the variance of the distance-matching Gaussians in the EC units was taken to be $\sigma_L^2 = 1.5^2$. These units also used threshold of $, _{EC} = 0.6$. As shown in proposition 1, these choices allow the EC cells to respond to landmarks within a circular region of radius 1.5 units from the EC field center. The activation threshold of CA3 units was also taken to be $, _{CA3} = 0.6$, which produces place fields roughly the same size as the EC fields. Finally, the threshold for the Mahalanobis distance test in the CA1 layer was taken to be 4.61. The rationale for this is provided in proposition 7.

The robot collects sensory inputs at 10 positions along its circular trajectory, and learns these places using the algorithms described above. We assume that the robot only senses and represents the landmarks shown. At each step, the robot moves in a straight-line fashion to the next place on its trajectory. However, motion errors, modeled as zero-mean Gaussians with standard deviation $\sigma_M = 0.5$, lead the robot away from its intended position.

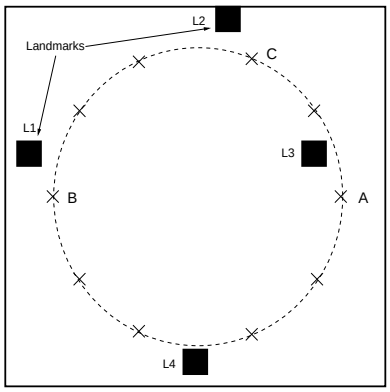

Figure 5: The simulation environment with four identical landmarks. With sensor range limited to 5 units, positions A, B, and C produce the same sensory inputs.

After the robot completes 20 turns on its circular trajectory, it is kidnapped from position A and introduced at position B. Thus, the robot is physically at position B but its dead-reckoning estimates are that of position A. Further, position C should be kept in mind, since with limited sensor ranges, all three places A, B, and C turn out to be perceptually identical. When kidnapped, the robot sets the variance of its position estimate to infinity, thus completely distrusting its dead-reckoning estimate. It also resets all the covariances between its position estimate and the place field centers to zero, thereby accepting its learned map as an accurate source of information. After these changes, it simply follows the Kalman filtering based spatial localization approach, which automatically leads to accurate localization of the robot based on sensory input.

We will now describe the experiments performed with this simulated model.

10.2 Experimental results

This section presents the results of our simulation experiments. The first experiment presents results assuming that the sensory range of the robot covers the entire room, thus, all the landmarks are always visible. In the second set of experiments, we consider the effects of limited sensor range, in which case the landmarks are not always visible. Since all the landmarks are identical, this leads to localization problems since multiple places appear perceptually alike. However, we will demonstrate that our place-based localization system allows the robot to localize and relocalize accurately.

10.2.1 Experiment 1: complete sensor range

In this experiment, the sensor range of the robot was assumed to be $R = 50$ units. Thus all the landmarks are visible to the robot if it is in the 20×20 region shown in Figure 5. Figure 6 shows a typical run of our robot simulation. Frame A in the figure shows the start position of the robot and the state of its spatial information which only includes one place unit. The circle shown in the figure represents the 2.5σ boundary, where σ is the uncertainty associated with the place field center and is given by the expression in proposition 2. The rationale for drawing the 2.5σ boundary is provided in proposition 8. Frame B shows the state of the robot spatial map just before it completes its first turn. The uncertainty on the robot position estimate is shown by the dotted circle while the complete circles denote the uncertainties associated with the place field centers. Although it is hard to see, without any revisits (and hence updates), the uncertainty of the place field centers steadily increase with each successive place visited by the robot. The $\mathbf{x}$ denotes the estimated center of the place field while the $+$ denotes the true center, i.e., the actual position of the robot when the corresponding place cell was recruited. As can be seen, these are rather close. Frame C denotes the effect of the robot revisiting the start position. In this case the Kalman filter updates are applied to the robot position estimate and the place field centers, thereby increasing their precision (decreasing the radius of the plotted circles). Frame D shows the system state after 10 turns while frame E denotes the system state after 20 turns. As can be observed, the uncertainty in place field centers learned by the robot decreases indicating that the robot has learned a robust metric representation of places on its circular trajectory. Frame F shows the trajectory followed by the simulated robot during its twenty turns. The effect of motion errors can be observed in the robot trajectory.

After 20 turns, the robot is kidnapped from position A and introduced at position B, as explained earlier and shown in Figure 5. Thus, the robot still has the position estimate of A although it is physically located at position B. We assume that the robot knows it has been kidnapped, hence it sets its position estimate variance to infinity (completely distrusting its position estimate). Thus, all CA1 units corresponding to the winning CA3 unit are bound to pass the Mahalanobis test. In such cases, a particular CA1 unit may be chosen as the winner either randomly or based on the least Mahalanobis distance. In our implementation, we choose the winner randomly. Frame A of Figure 7 shows that the sensory inputs permit the robot to identify the place correctly as position

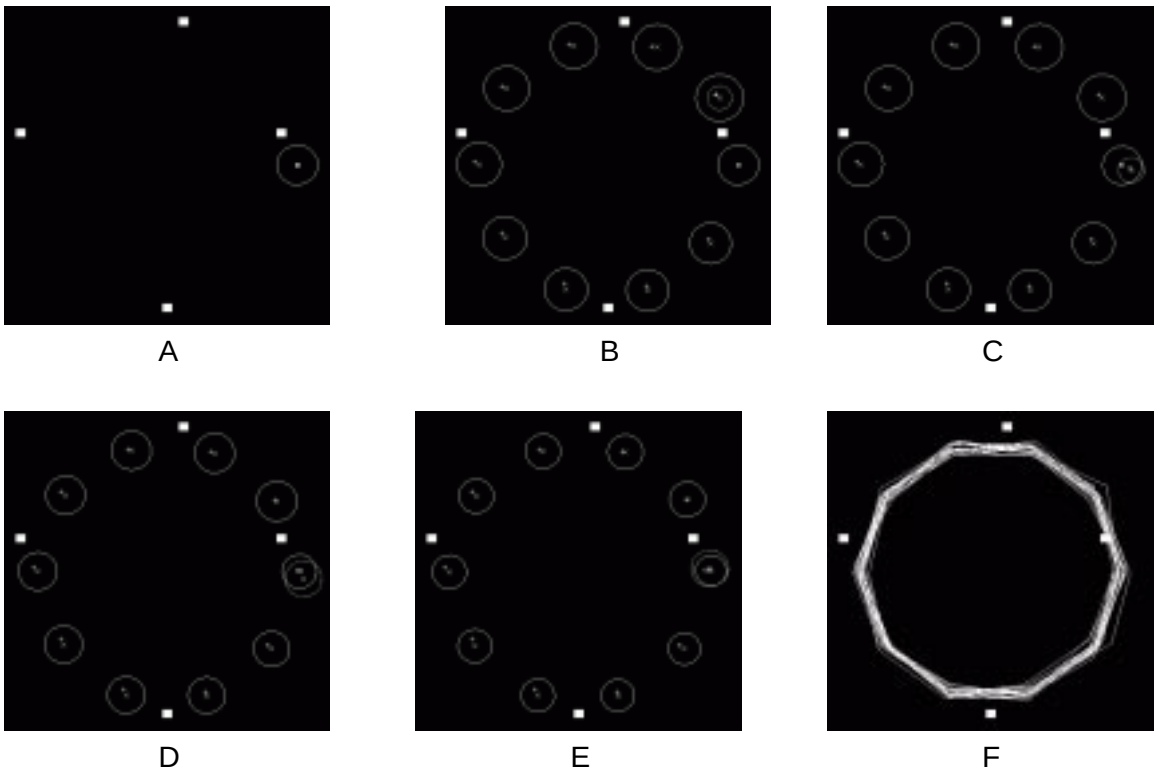

Figure 6: With sensor range R=50 units. Robot starts at the position shown in frame A and executes a clockwise circular trajectory consisting of 10 places where sensory observations are performed. Frame F shows the robot trajectory over 20 turns. (See text for other explanations.)

B. The Kalman filter updates then correct the robot position estimate to that of position B and the robot localizes correctly in the very first step. This localization is aided by the fact that the unlimited range of the sensors produce *unique* places in the environment. In experiment 2 we will consider robot localization under more challenging conditions (limited sensor ranges).

Owing to the initial large variance of the robot position estimate, the updated variance, although decreasing, is still rather large, as shown in frames B, C, D, F, and G of Figure 7. Frame H shows the state of the system when the robot completes one turn after being kidnapped and reintroduced, while frame I is the state of the system after 10 turns. As can be observed, the uncertainty associated with the robot position estimate reduces considerably. Thus, using the place-based Kalman filtering approach, the robot is able to localize correctly even if it is kidnapped and reintroduced at a different location.

Figure 8 shows some of the firing properties of our neural model. Frame A shows the firing field of EC unit 0, with the firing strength increasing from the boundary towards the center (as

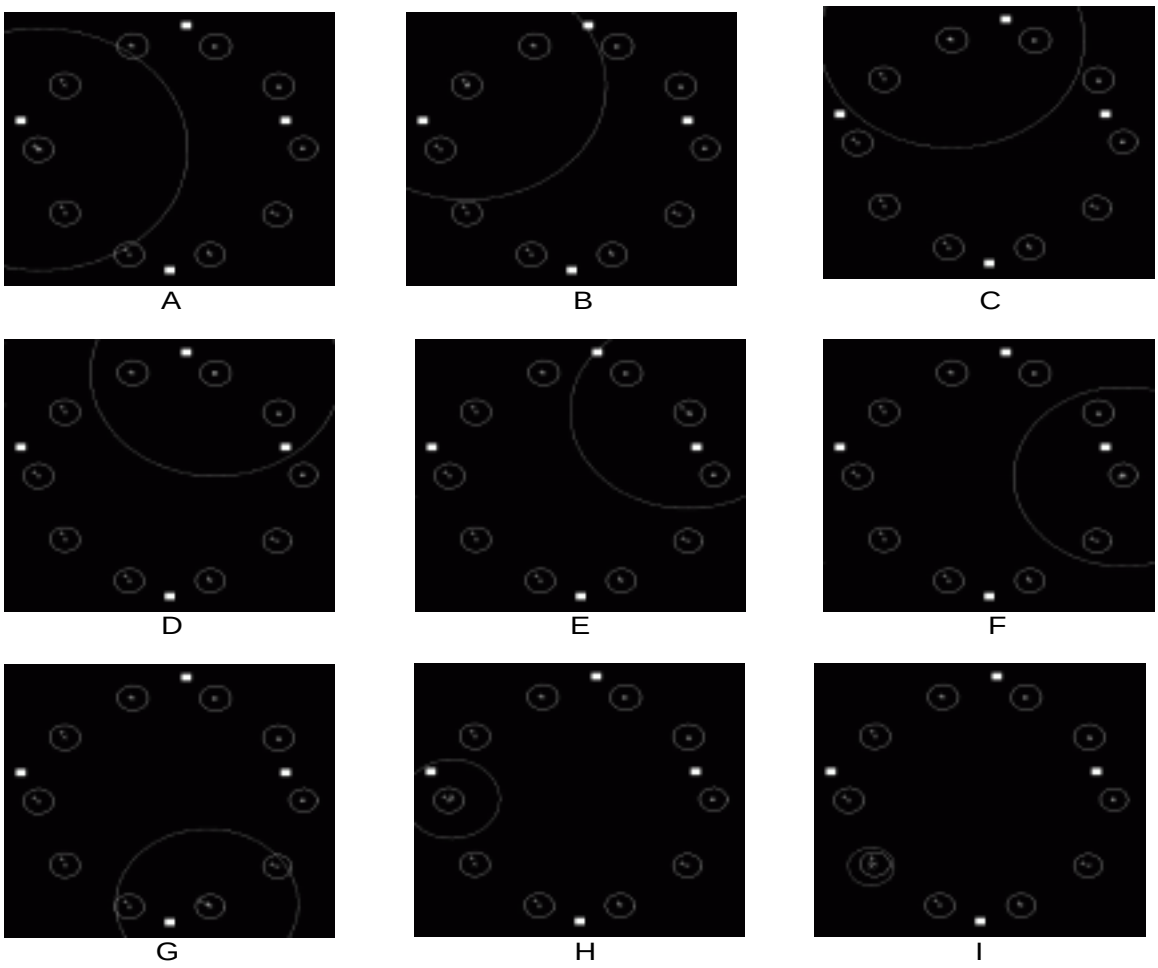

Figure 7: With sensor range R=50 units. The robot is kidnapped and introduced at a different location. Based on sensory information the robot localizes correctly. (See text for other details.)

mentioned earlier, this field is a Gaussian). This unit fires maximally when the robot observes a landmark 9 units north and 7 units west of its current position. Similarly, frame B shows an EC unit that responds to a landmark 2 units north and 1 unit west of the robot position, while frame C shows an EC unit responding to landmarks appearing 8 units to the west and 8.8 units to the south of the robot position. Frame D shows the firing of CA3 unit 0, which shows that the unit fires in a unique region of the environment. Indeed, with unlimited sensor ranges, all the places in the environment turn out to be unique. Thus, the number of CA1 and CA3 units were observed to be equal: one CA1 unit for each CA3 unit, as shown by the firing of CA1 unit 0 in frame E.

Frame F in the above figure shows the place field map, i.e., the firing of CA1 cells. The size of these fields is determined by the firings of the EC cells, which are dependent on the values of σ_L and σ_S in our model. Since the place cell firing is a result of EC firing and we have chosen the

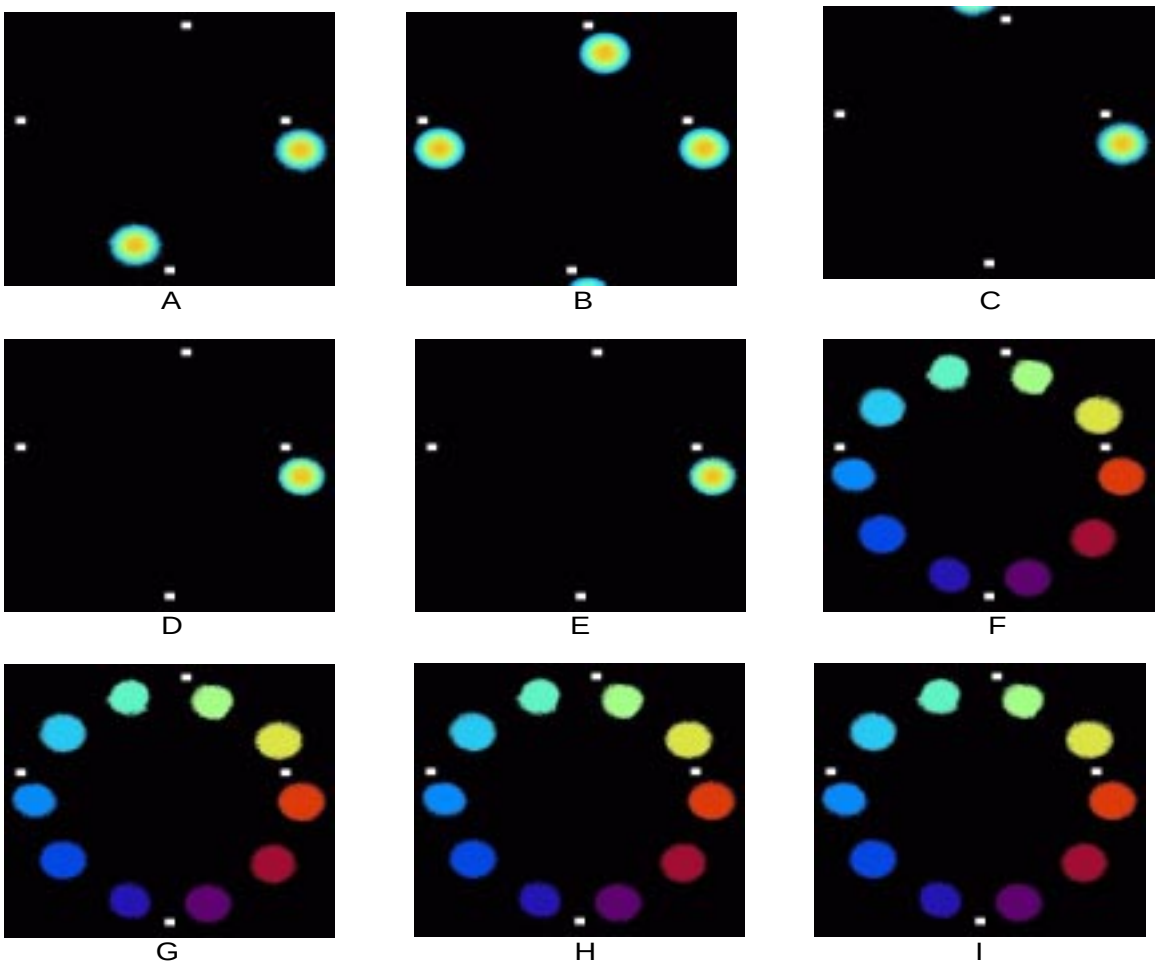

Figure 8: With sensor range R=50. Frames A, B, and C show the fields of EC units 0, 1, and 2. Frame D shows the firing field of CA3 unit 0, while Frame E shows the corresponding firing field of CA1 unit 0. The place field map (all CA1 units) is shown in F, G, H, and I. (Refer to the text for further details.)

CA3 activation threshold to be the same as the EC activation threshold, the place fields are equal or smaller in size than the EC fields. Further, the place fields are largely circular since the sensor ranges are unlimited. Frames G and H show the place field map after the robot is kidnapped and reintroduced. As can be observed, apart from minor movements of place field centers (and hence the place field's), there is not much change in place field firing. Frame I shows the place field map after the reintroduced robot completes 10 turns.

10.3 Experiment 2: limited sensor range

The above experiment demonstrated the ability of our model to learn places and localize correctly even when the environment contained identical landmarks. However, to a large extent this was easy because of the assumption of unlimited sensor ranges. In this experiment, we consider the scenario where the sensors have limited ranges. If the environment contains many identical landmarks, this restriction leads to *perceptual aliasing*, i.e., produces similar sensory inputs at different places in the environment.

Frame A in Figure 9 shows the state of the system at the start of the simulation. Note that the 2.5σ boundary is much smaller in this experiment as compared to the one before. This is because the sensing error is given by $R^2\sigma_S^2$ and $R = 5$ units in this experiment (compared to 50 in the previous one). Frame B shows the state of the system before the completion of one turn. A few observations can be made here. First, the increase in the uncertainty (and hence the corresponding increase in the size of the circles) can be easily noticed. Second, the limited sensor ranges of the robot deprive it of sensory information (i.e., the robot is *sensor blind*) at two places in its trajectory. Hence, the spatial learning system does not recruit any place cells at these positions. Frame C shows the completion of one turn and the corresponding decrease in the state estimate uncertainties. Frame D shows the system state after 10 turns. Notice that the robot has added a second place field in the north-west quarter of its trajectory. This happened because the motion error led the robot to a place where the CA3 firing was marginally below the activation threshold, forcing the system to create a new place cell. Frame E shows the system state after 20 turns, while the robot trajectory over the 20 turns is shown in frame F.

As before, the robot is kidnapped from position A after 20 turns and reintroduced at position B. However, unlike the earlier case the limited sensor ranges in this experiment produce identical sensory information at positions A, B, and C shown in Figure 5. Thus, although the reintroduced robot is physically at position B and has the position estimate of position A, the localization system determines the winner as the place corresponding to position C. Frame A shows the result of the Kalman filtering based localization process, which updates the robot position estimate to that of position C. This is a wrong localization since the robot is actually at position B. Frame B shows the state of the system after one movement step by the robot. Based on the wrong localization of frame A, the system now thinks it is at a totally new position (outside the boundary of the

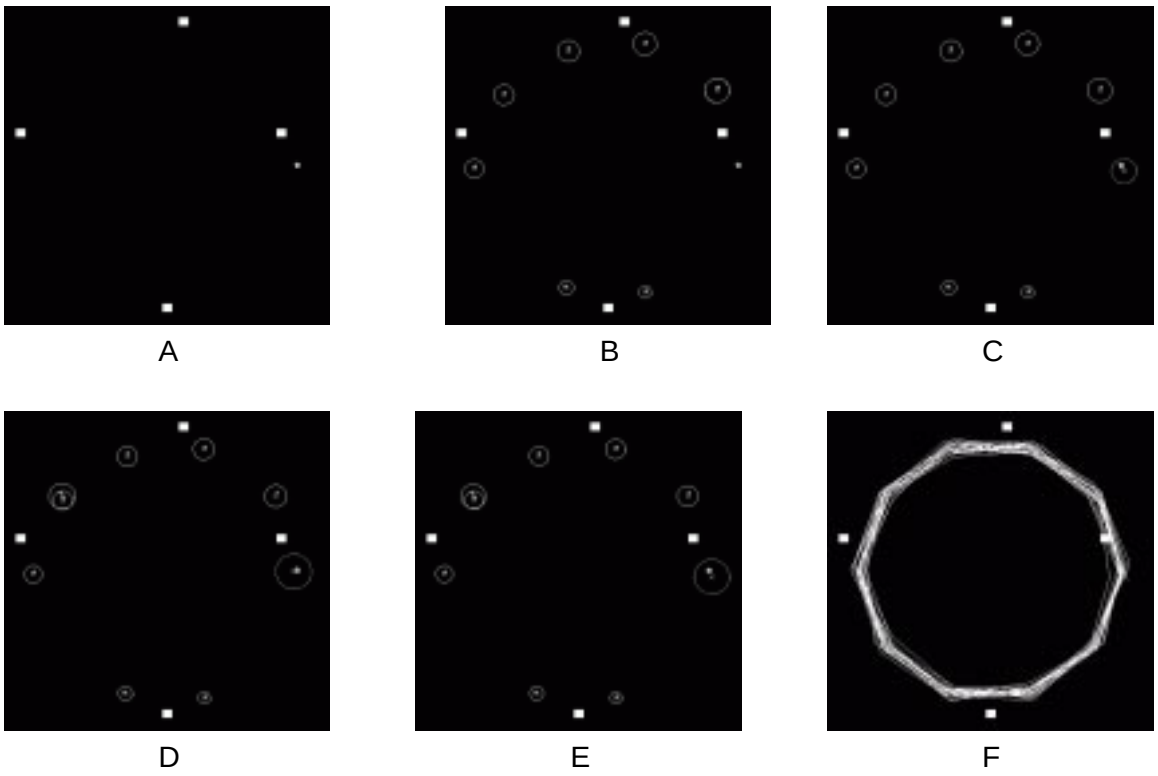

Figure 9: With sensor range R=5 units. Experiment with limited sensor ranges. The evolution of the state of the system with robot motion is shown. Notice that with limited sensor ranges, two places in the trajectory are sensorially deprived. (Other details appear in the text.)

figure shown) and creates a new place unit as shown in frame B. Similarly, the next two robot motions also result in the creation of new place units (all of them located outside the region shown in the figures), and are shown in frames C and D. Frame E shows that the robot finally reaches a place where the sensory input corresponds to a place visited earlier, and importantly, it also passes the Mahalanobis distance test. Thus, the robot relocalizes to this place, with the Kalman updates making appropriate changes to the place units recruited after reintroduction. Frames F and G show further improvement in robot localization, which by now is quite accurate. Frame H shows the system state at the end of one turn. Notice that the centers of the place cells that were recruited incorrectly have been slowly updated to correspond to the correct locations. Frame I shows the result after 10 turns. As can be seen, except for one place cell, the other wrongly recruited cells have been updated to correspond to the correct place field centers. Thus, not only has the robot localized correctly but has also corrected its initial localization error.

Figure 11 shows the particulars of the firing fields. Frame A shows the firing field of EC unit 0,

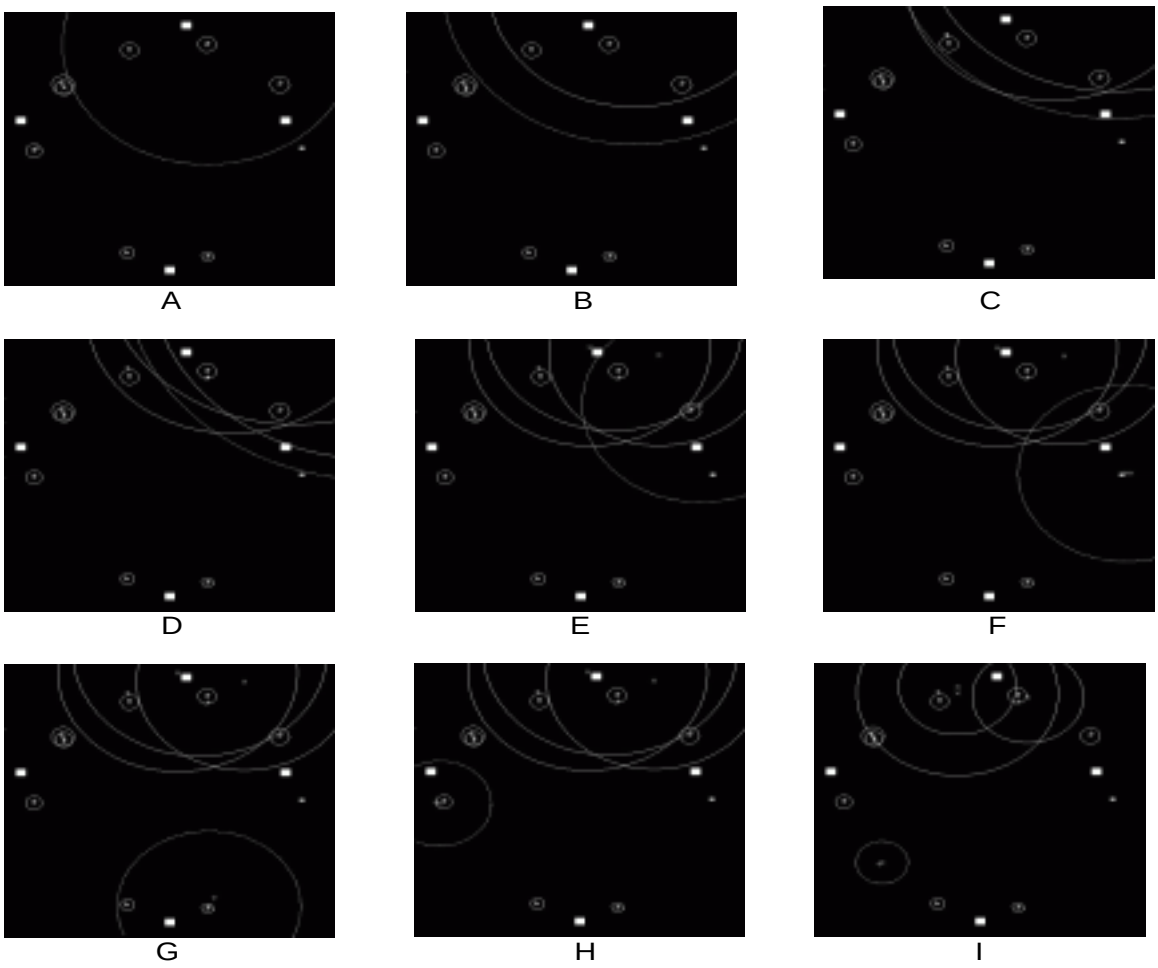

Figure 10: With sensor range R=5 units. The kidnapped robot problem with limited sensor ranges. Upon introduction, the robot localizes wrongly as shown in frames A, B, C, and D. Finally the robot corrects is initial mistake, as shown in frame E. Updates of the model parameters allow the robot to localize faithfully and also correct its place field estimates, as shown in frame I. (Other details appear in the text.)

which responds to landmarks appearing 1 unit to the west and 2 units to the north of the robot. Frame B shows the properties of EC unit 1, which responds to landmarks appearing 1 unit to the west and 0.5 units to the south of the robot, while frame C shows EC unit 2 responding to landmarks 2 units to the east and 0.5 units to the south of the robot position. Frame D shows the different places in the environment over which CA3 unit 0 responds. As can be seen, there are multiple places that appear perceptually identical to the robot, in this case, corresponding to positions A, B, and C of Figure 5. Frame E shows the firing of CA1 unit 0. Note that although the CA3 unit 0 fires at multiple locations, the CA1 unit only fires at one location, a result of the Mahalanobis distinguishing test. The place field map at the end of 20 turns is shown in frame F

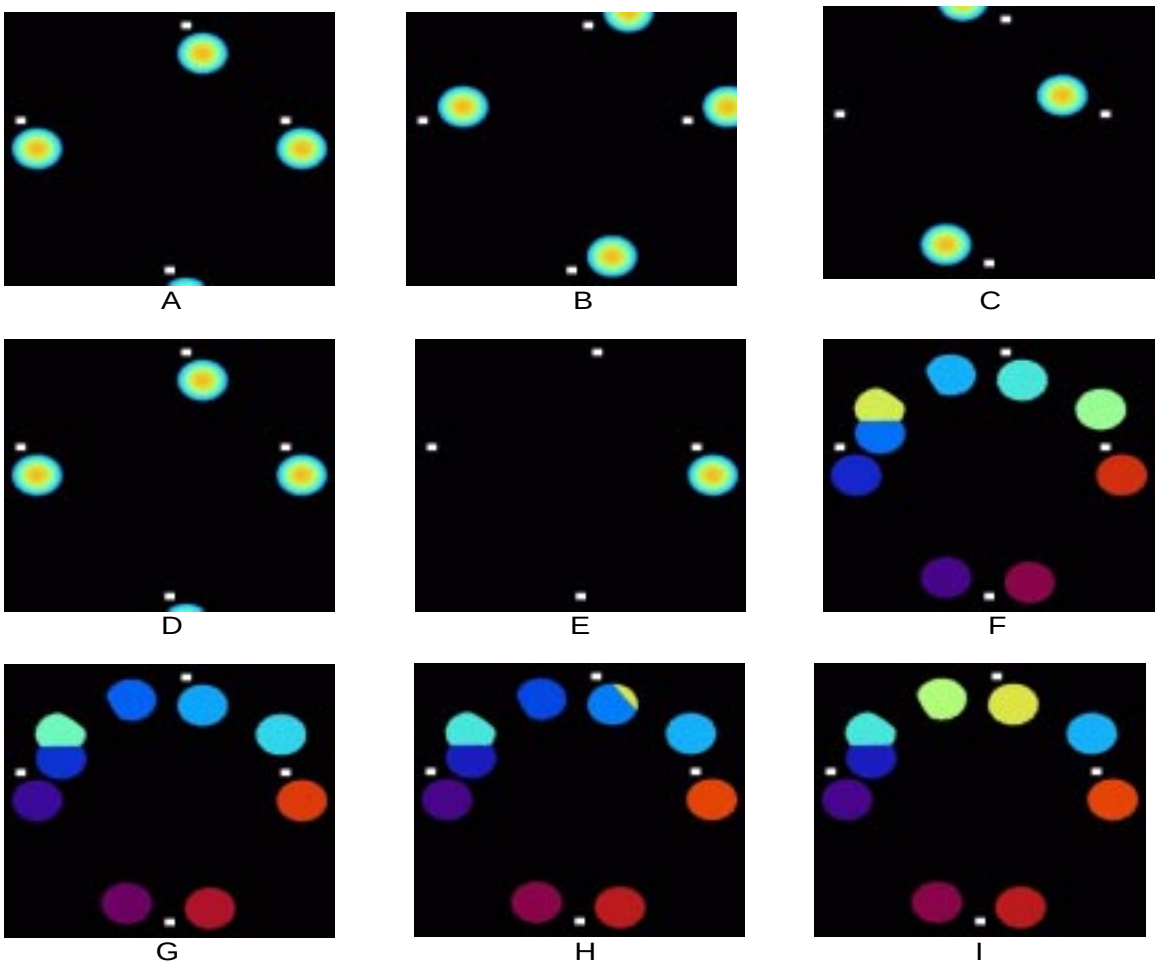

Figure 11: With sensor range R=5 units. Firing fields of EC units 0, 1, and 2 are shown in frames A, B, and C. Frame D shows that multiple places excite CA3 unit 0 (perceptual aliasing). Frame E shows that CA1 unit 0, only responds to one of the places that activate CA3 unit 0. Place field maps are shown in F, G, H, and I. (Refer to the text for other details.)

of Figure 11. Note that some of the place fields are not circular, a product of the limited sensor ranges. Frame G shows the place field map after the reintroduction of the robot. Although it appears identical to frame F, there is another place cell that is located outside the display region. Frame H shows the place field map after the robot has localized correctly as explained earlier. Thus, this map corresponds to the system state in frame G of Figure 10. As can be seen, Kalman filtering updates make the wrongly recruited cells slowly blend into the corresponding correct ones. Frame I shows the place field map after 10 turns of the robot. As can be observed, the incorrect place cells have blended in completely, but for one that is overshadowed by another cell shown in Frame I of Figure 10.

11 Related work

Since localization plays a critical role in robot navigation, it is hardly surprising that numerous techniques have been developed for robot spatial learning and localization. Among these, the ones that bear close relation to the localization system described in this paper can be broadly divided into three categories: (1) Probabilistic and uncertain information fusion approaches related to Kalman filtering (2) Topological approaches based on cognitive mapping theories, and (3) Neurobiological models of spatial learning and localization. We will briefly discuss and compare each of these approaches with our model.

11.1 Approaches related to Kalman filtering

Since robots perceive aspects of their environments through their sensors, any attempt at world-modeling must be preceded by sensory information fusion (also called sensor fusion). Smith and Cheeseman argued strongly for the use of Bayesian estimation theory in robot spatial representation (the *stochastic map*) (Smith *et al.*, 1990), and showed that an *optimal* information fusion approach was equivalent to a simple form of Kalman filtering (Kalman, 1960). While the *extended Kalman filter* framework for building 3D maps of the environment was developed by (Ayache & Faugeras, 1987), a *generalized filter* approach was developed by (Moutarlier & Chatila, 1989) to perform estimation and fusion of uncertain sensory information. A detailed presentation of the Kalman filter approach to robot localization appears in (Crowley, 1995), while the necessity and difficulties associated with maintaining correlations of the state variables of a stochastic map are detailed in (Hebert *et al.*, 1995). Some other probabilistic localization approaches, not directly related to Kalman filtering, appear in (Dorst *et al.*, 1995; Thrun, 1996).

The Kalman filtering approaches for robot localization require a *sensor model of the environment* in the measurement function. This sensor model provides the sensory inputs (or measurement) that the robot would receive when in any given position. Conventional approaches use a measurement function that specifies the *relative positions* of landmarks with respect to the robot. In such cases, the landmarks are represented in a robot-centered frame and the landmark positions are updated based on robot motion. These updated positions serve as predictions while the observed positions of the landmarks serve as observations (Smith *et al.*, 1990; Ayache & Faugeras, 1987; Leonard & Durrant-Whyte, 1992; Moutarlier & Chatila, 1989; Crowley, 1995), making Kalman

filtering possible.

However, if the environment contains multiple identical landmarks and sensor ranges are limited, this measurement function leads to matching problems (i.e., which state vector element should the sensed landmark be matched against?) when the robot is kidnapped and reintroduced at another place. In contrast, the model described and implemented in this paper performs *place-based* localization. Since places are more distinct (and distinguishable) than relative landmark positions, it is easier to relocalize with a place-based system. This has led some researchers to suggest place-based extensions of Kalman filtering approaches (Crowley, 1995; Hebert *et al.*, 1995).

Another key distinction of our model is that it does not require an explicit sensor model (apart from the simple neural system for recognizing places). By labeling places with dead-reckoning inputs, the system develops a kind of *inverse sensor model* that produces a place code (and a position estimate) in response to sensory input. This position estimate is used by the probabilistic localization process.

11.2 Topological approaches based on cognitive mapping theories

Tolman proposed that animals and humans form an internal representation of the environment, which he called a *cognitive map* (Tolman, 1948). Since then, many researchers have developed theories of cognitive mapping (Kaplan, 1973a; Kaplan, 1973b; Kuipers, 1978). Based on two primary insights concerning cognitive maps: criticality of a *topological* description of the environment, and the grounding of the spatial representation in the *sensorimotor* interactions between the agent and the environment, Kuipers proposed a three level representation of space called the *spatial semantic hierarchy* (SSH). The lowest level consists of control rules that define *distinctive places* as some property of sensory inputs. The next higher level creates a topological representation by linking distinctive places by *travel edges*. The highest level in the hierarchy contains a *geometric representation* of the robot's sensory environment (Kuipers & Byun, 1991). This cognitive spatial learning architecture was implemented on a simulated robot NX (Kuipers & Byun, 1991) and later extended to physical robots (Kuipers *et al.*, 1993).

Kortenkamp's RPLAN is an implementation of the PLAN model of a human cognitive mapping (Chown *et al.*, 1995; Kaplan, 1973a; Kaplan, 1973b). In his implementation, sonar-based detection of *gateways* and vision-based detection of *scenes* are combined using a Bayesian network to provide robust definitions of place. The system then uses these place definitions to construct a topological

map representation of the environment (Kortenkamp, 1993; Kortenkamp & Weymouth, 1994).

Cognitive mapping theories have also inspired multi-level space representations. For instance, Qualnav, a simulated robot (Levitt & Lawton, 1990) uses a multi-level spatial representation. At the lowest level, relative angles and estimated distances to landmarks define regions of space called *viewframes*. At the next higher level, pairs of landmarks are used to define a virtual boundary called the *landmark pair boundary* (LPB). These LPBs lead to a topological division of space called *orientation regions*. Together, these two approaches allow for specific localization of the robot using viewframes within more general orientation regions.

The models described in this section are based on cognitive theories of animal and human spatial learning. Our model, on the other hand, is based on neurobiological data. Thus, the models described here provide implementations of abstract theories of spatial representation and manipulation, while our model attempts a computational characterization of a particular brain region (the hippocampus). However, it is interesting to observe that the SSH hierarchy of Kuipers bears close resemblance to the information representation suggested in our computational model (section 6).

11.3 Neurobiological models of robot navigation

Some neurobiological models of spatial learning have also been implemented on mobile robots. Mataric implemented a topological *place graph* (Mataric, 1992), loosely based on the place unit model of McNaughton and Nadel (McNaughton, 1989; McNaughton & Nadel, 1990). Using her model, the robot Toto explored the environment and built a topological graph. The nodes in the graph represented *landmarks* and the links encoded the robot motions. Places in the model were associated with individual landmarks like walls, corridors, etc. Once the map was built, goal-directed navigation was performed by *spreading activation* backwards from the goal node and following the path to the *strongest activated* neighbor of the current node. Thus the model implements topological navigation and is incapable of determining novel routes or short-cuts (Mataric, 1992).

Bachelder and Waxman have also implemented a spatial learning system on a mobile robot called MAVIN (mobile adaptive visual navigator). This robot wanders around the environment recognizing places based on the configuration of landmarks visible from that location (Bachelder & Waxman, 1994). Landmarks are recognized using a Seibert-Waxman neural 3D object recogni-

tion system (Seibert & Waxman, 1992) which is trained to recognize the landmarks prior to the exploration by the robot. As the robot moves, an associative neural network learns the movements that lead from one place to another, using a Hebbian rule. Although this model learns places and recognizes them later in spite of viewing errors and self-motion uncertainties, it does not include any path planning abilities (Bachelder & Waxman, 1994).

Recce and Harris have implemented a robot navigation system based on interactions of neorcortical and hippocampal theories (Recce & Harris, 1996). According to their theory, the hippocampus functions as an *auto-associative* memory for matching *ego-centric* maps which are constructed in the neocortex. The hippocampus stores snapshots of this ego-centric map and the activity of head-direction cells are used to determine the best map rotation to match the snapshots stored in the hippocampus (Recce & Harris, 1996). Using a mobile robot with sonar sensors, they have tested an implementation of their theory.

The approaches described in this section deal with topological space representations. Further, even though the models were implemented on real robots, none of the models have explicit mechanisms to handle sensory and motion errors. In contrast, our model builds a metric representation of space and explicitly performs fusion of uncertain information.

12 Discussion

In this paper we have described a computational model of hippocampal function from the point of view of spatial learning. The primary thesis of this paper is that the hippocampal system learns places and associates them with dead-reckoning estimates, thereby learning a metric map of the environment. This metric representation allows the animal to navigate to arbitrary goals and locations on a direct trajectory. However, in order for such a representation to exist, the dead-reckoning estimates of the animal must be faithful and reliable, even in the face of perceptual aliasing (when multiple places appear sensorially identical). Further, since the sensory and dead-reckoning input streams can have uncertainty associated with them, it is also imperative that the model be capable of handling such uncertainties.

Based on the parallel between the requirements of our computational model and the Kalman filtering approach for probabilistic robot localization, we developed a Kalman filter framework for our localization model. Not only does this approach handle uncertain data it also provides

stochastically optimal rules for information updates in the model. The model learns places based on sensory data, and through the Kalman filter process also attempts to learn the dead-reckoned coordinates of the place field centers. Using a related tool, the Mahalanobis distance, the system is capable of distinguishing between perceptually similar places. The place field centers as well as the current dead-reckoning position are represented by estimates with associated covariances that are updated appropriately when the animal visits or revisits places. With frequent revisits to a known place, the uncertainty associated with that place field center can be seen to decrease and the estimated place field center converges towards the true center. Further, the system handles relocalization (kidnapped robot problem) very easily by setting the variance of the robot's postion estimate to infinity and using the same Kalman filter approach.

Although we haven't shown any results to this effect, goal-directed navigation is easily realized in our system. Goals encountered by the animal are assumed to be represented in terms of their locations. These locations are computed from the animal's dead-reckoned estimate and the position of the goal relative to the robot. Once such locations are learned, the robot can directly navigate to any goal location by computing a vector-difference of the goal position and its current position. Thus, our current implementation allows the animal to perform metric navigation.

Our model differs significantly from the other implementations (Wan *et al.*, 1994; Prescott, 1995; Redish & Touretzky, 1996) of metric spatial representation in the hippocampus. The key contributions of our model include the suggestion of specific *computational roles* to the hippocampal regions, including the suggestion that the CA1 layer resolves perceptual aliasing problems based on dead-reckoning input. Although the sensory and dead-reckoning systems are prone to errors, calling for probabilistic approaches for information fusion, they have not been addressed in the other models. Finally, our hippocampal characterization concedes that a multi-level representation of spatial information exists in the hippocampus, namely: directional, topological, and metric, although this aspect has not yet been realized in a computational form.

Our model makes some key neurobiological and behavioral predictions that are elaborated elsewhere (Balakrishnan & Honavar, 1997a). For instance, our model predicts that perceptually identical places in the same environment will excite the same population of cells in the CA3 layer but different populations in the CA1 layer. Also, the drifts in CA3 and CA1 firing in darkness can possibly be different since they are maintained by different motion sources in our model. Our model also predicts that animals can reduce their computational complexity of localization by navigating

either randomly or from one place field center to another. A related behavioral prediction is that an exploring animal will search in gradually expanding trajectories, since this allows the propagation of reliable dead-reckoning estimates further and further away from its starting position (Balakrishnan & Honavar, 1997a). Some possibilities for the neural basis of such computations have also been put forth. We have suggested that the matrix inversions required in the computation of the Kalman gain and the Mahalanobis distance might be performed in the CA1 layer through an iterative mechanism (O'Keefe, 1989), while the propagation of covariances might be related to the *sharp waves* observed in resting rats (Buzsaki, 1989).

12.1 Assumptions in our model

Some key assumptions have to be made for our computational model to be realizable. These assumptions are clarified in this section.

1. **Recognized landmark information**

   Our model assumes that the EC inputs consist of recognized landmarks along with information pertaining to their allocentric position relative to the robot. Our model required this because of its analogy to the hippocampal formation, which is known to derive highly processed inputs from other associational areas of the brain. Since object and scene recognition are still big problems in contemporary robotics, is this approach only a simulation toy that is unimplementable on real robots? We suggest not. It might be observed that the functioning of our localization system depends on the notion of a place but does not depend on the exact mechanisms for defining a place representation. Thus, any prudent choice of a place representation would work. For e.g., a *local occupancy-grid* representation of a place can be used in our model, making it implementable on a mobile robot with sonar sensors. Such representations have been successfully used (Langley & Pfleger, 1995; Recce & Harris, 1996; Yamauchi & Langley, 1997).

2. **Reliance on dead-reckoning**

   The model discussed in this paper assumes that the robot has a reliable dead-reckoning system with known error models. Dead-reckoning in contemporary robots is usually performed through odometric techniques that use optical and magnetic wheel encoders. Since the odometric approaches derive their navigational parameters from wheel rotation, they are subject

to problems arising from slippage, tread wear, and/or improper tire inflation (Balakrishna & Ghosal, 1995; Everett, 1995). However, Doppler and inertial navigation systems can often be used to considerably reduce these sources of errors (Everett, 1995). *Doppler navigation* systems operate on the principle of the Doppler shift in frequency, observed when radiated energy reflects off a surface that is moving with respect to the emitter. *Inertial navigation* systems rely on a set of mechanisms that continuously sense minute accelerations in each of the three directional axes. These are then integrated over time to yield velocity and position. Such systems, although capable of producing reasonably precise dead-reckoning, currently have limited applications owing to their prohibitive cost (Everett, 1995). However, with advances in technology, it is conceivable that accurate and affordable dead-reckoning devices will soon become available, making our approach quite practical.

3. **Maintaining correlations**

   With probabilistic localization approaches like the Kalman filter, it is imperative that the correlations between the state variables be maintained correctly. Estimating and maintaining these correlations is often difficult owing to the approximation errors stemming from linearizing the (usually) non-linear system and measurement functions, biases on the robot position, and the computational complexity associated with updating state vectors containing a large number of elements (Hebert *et al.*, 1995). However, these correlations and variances cannot be neglected since doing so will lead to inconsistencies on the uncertainties (Hebert *et al.*, 1995). In our model, we ignore the autocorrelation of the measurement noise. However, as we argued before, if the animal navigates randomly or purposefully between place field centers, this correlation term will be negligible.

12.2 Contributions to robot localization

The model described and implemented in this paper makes some interesting contributions to robot localization.

1. This paper provides an implementation of a neuro-cognitive model of animal spatial learning and localization. By describing the model in a Kalman filter framework of probabilistic robot localization, this paper makes the model easily implementable on physical robots.

2. From another angle, the model in this paper is a *place-based extension* of the Kalman filtering approach to robot localization. Instead of estimating and updating landmark positions in a robot-centered frame, our approach defines *places* and estimates the centers of these places. This produces a compact representation of the environment since only distinct places are represented. Additionally, these places are labeled with metric information. Thus, this model includes advantages of metric as well as relational representations of space.

3. Places are defined based on landmark configurations sensed from that place, and a simple neural model is used to map the sensory inputs into place codes. The centers of these places are labeled with dead-reckoning based position information. Crudely, this can be thought of as an *inverse sensor model* that produces a place code (with its associated position estimate) in response to sensory input.

4. The model also includes a simple solution to the perceptual aliasing problem with dead-reckoning being used to distinguish between perceptually identical places. Although this idea is not new to robotics, it fits very well with the neuro-cognitive model we have described.

5. Place-based localization and the ability to disambiguate between perceptually similar places makes this approach very robust. This approach can thus localize in environments with many identical landmarks using sensors of limited range.

6. Importantly, our model allows the robot to *relocalize*. Thus, if the robot is kidnapped from one location in the environment and reintroduced at another, it can faithfully localize provided: it can sense that it has been kidnapped and it is reintroduced at a place (or near a place) it has visited before. Pure dead-reckoning based systems cannot localize after being kidnapped (Yamauchi & Beer, 1996) while pure sensory based systems will localize incorrectly if perceptual aliasing exists.

In addition to the contributions summarized above, our characterization of the hippocampus supports a few additional capabilities which are yet to be implemented. For instance, although powerful mechanisms exist for handling the precisions of the estimates in robot map learning and localization (Kalman filter and other probabilistic approaches), there is little theory in robotics for handling the *confidence* of the represented or observed objects (Leonard & Durrant-Whyte, 1992; Crowley, 1995). Note that while variances characterize the imprecision or uncertainty associated

with the *value* of some object (or variable), confidence denotes the *likelihood of the existence* of the object. For instance, an uncertainty might be associated with the position of a landmark but a confidence signifies whether the landmark was indeed observed. In our model, the connections between the CA3/EC and CA3/Dg are in a prime position to serve as these confidence factors. Further, since these connections are modifiable, the update of these weights can signify an increase or decrease in the confidence of an object. Thus, with an appropriate learning mechanism, our model can function in dynamic environments (i.e., environments where objects move).

12.3 Work in progress

The model described and implemented in this paper can be extended in a several different ways, some of which are currently being explored.

1. As explained above, dynamic environments (where objects move) require a characterization of the *confidence* i.e., the likelihood of an object being present in a particular position (in addition to the uncertainty associated with its exact position of the object). As we suggested earlier, the synapses between Dg/EC and the CA3 cells in our model can possibly play a role in establishing the relative confidences in the observed objects. If this happens to be the case, then synaptic changes can allow the system to update its confidence in the presence or absence of particular objects, thereby allowing it to cope with dynamic environments.

2. We believe that the CA3 region encodes a topological map of the environment. Since the CA3 collaterals predict the place that the robot will be in after executing its current motion and the sensory system provides an observation of a place, it appears that the CA3 region, by itself, functions as a predict-observe-match-update system. Further, since the motion information hypothesized to be encoded in the collaterals is derived from motor efference copies (and is prone to errors), principles of Kalman filtering can be extended to this role of CA3.

3. Similarly, our current belief is that the Sb learns a few key places in *egocentric* terms. Since such places will only be recognized when the animal is at a particular place and faces a specific direction, these places implicitly contain *directional* information (as opposed to the CA3 and CA1 place cells which are considered non-directional). These places are associated

with the animal's current head-direction in the postsubicular head-direction cells. Thereupon, a disoriented animal can recognize an egocentric place in the Sb place cells and recall the associated head-direction from the postsubiculum. Since this system also behaves in a predict-observe-match-update manner, it too, can be approached with Kalman filtering theory.

References

Abraham, L., Potegal, M., & Miller, S. (1983). Evidence for Caudate Nucleus Involvement in an Egocentric Spatial Task: Return from Passive Transport. *Physiological Psychology*, **11**(1), 11–17.

Anderson, E. (1983). *Animals as Navigators*. Van Nostrand Reinhold Company.

Ayache, N., & Faugeras, O. (1987). Maintaining Representation of the Environment of a Mobile Robot. *In: Proceedings of the International Symposium on Robotics Research.*

Bachelder, I., & Waxman, A. (1994). Mobile Robot Visual Mapping and Localization: A View-Based Neurocomputational Architecture that Emulates Hippocampal Place Learning. *Neural Networks*, **7**, 1083–1099.

Balakrishna, R., & Ghosal, A. (1995). Modeling of Slip for Wheeled Mobile Robots. *IEEE Transactions on Robotics and Automation*, **11**(1), 126–132.

Balakrishnan, K., & Honavar, V. (1997a). *Hippocampal Involvement in Probabilistic Localization: Is the Hippocampus a Kalman Filter?* (in preparation).

Balakrishnan, K., & Honavar, V. (1997b). Spatial Learning for Robot Localization. *Pages 389–397 of: Proceedings of the Second International Conference on Genetic Programming.* Morgan Kaufmann.

Barnes, C., McNaughton, B., Mizumori, S., Leonard, B., & Lei-Huey, L. (1990). Comparison of Spatial and Temporal Characteristics of Neuronal Activity in Sequential Stages of Hippocampal Processing. *Progress in Brain Research*, **83**, 287–299.

Biegler, R., & Morris, R. (1996). Landmark Stability: Studies Exploring Whether the Perceived Stability of the Environment Influences Spatial Representation. *The Journal of Experimental Biology*, **199**(1), 187–193.

Blair, H., & Sharp, P. (1995). Anticipatory Firing of Anterior Thalamic Head Direction Cells: Evidence for a Thalamocortical Circuit that Computes Head Direction in the Rat. *Journal of Neuroscience*, **15**, 6260–6270.

Blum, K., & Abbott, L. (1996). A Model of Spatial Map Formation in the Hippocampus of the Rat. *Neural Computation*, **8**, 85–93.

Bousquet, O., Balakrishnan, K., & Honavar, V. (1997). *Is the Hippocampal Formation a Kalman Filter?* (to appear in the Proceedings of the Pacific Symposium on Biocomputing'98).

Brooks, R. (1985). Visual Map Making for a Mobile Robot. *In: Proceedings of the IEEE Conference on Robotics and Automation.*

Brown, M., & Sharp, P. (1995). Simulation of Spatial Learning in the Morris Water Maze by a Neural Network Model of the Hippocampal Formation and Nucleus Accumbens. *Hippocampus*, **5**, 189–197.

Burgess, N., & O'Keefe, J. (1996). Neuronal computations underlying the firing of place cells and their role in navigation. *Hippocampus*, **6**, 749–762.

Burgess, N., Recce, M., & O'Keefe, J. (1994). A Model of Hippocampal Function. *Neural Networks*, **7**(6/7), 1065–1081.

Buzsaki, G. (1989). Two-State Model of Memory Trace Formation: A Role for "Noisy" Brain States. *Neuroscience*, **31**, 551–570.

Chen, L., Lin, L-H., Green, E., Barnes, C., & McNaughton, B. (1994b). Head-Direction Cells in the Rat Posterior Cortex. I. Anatomical Distribution and Behavioral Modulation. *Experimental Brain Research*, **101**, 8–23.

Chen, L., Lin, L-H., Barnes, C., & McNaughton, B. (1994a). Head-Direction Cells in the Rat Posterior Cortex. II. Contributions of Visual and Ideothetic Information to the Directional Firing. *Experimental Brain Research*, **101**, 24–34.

Chown, E., Kaplan, S., & Kortenkamp, D. (1995). Prototypes, Location and Associative Networks (PLAN): Towards a Unified Theory of Cognitive Mapping. *The Journal of Cognitive Science*, **19**(1).

Churchland, P., & Sejnowski, T. (1992). *The Computational Brain.* Cambridge, MA: MIT Press/A Bradford Book.

Cohen, N., & Eichenbaum, H. (1993). *Memory, Amnesia, and the Hippocampal System.* Cambridge, MA: MIT Press/A Bradford Book.

Collett, T., Cartwright, B., & Smith, B. (1986). Landmark Learning and Visuo-Spatial Memories in Gerbils. *Journal of Neurophysiology A*, **158**, 835–851.

Crowley, J. (1995). Mathematical Foundations of Navigation and Perception for an Autonomous Mobile Robot. *Pages 9–51 of: Proceedings of the International Workshop on Reasoning with Uncertainty in Robotics.* Springer-Verlag.

Dorst, L., van Lambalgen, M., & Voorbraak, F. (eds). (1995). *Proceedings of the International Workshop on Reasoning with Uncertainty in Robotics.* Springer-Verlag.

Elfes, A. (1989). *Occupancy Grids: A Probabilistic Framework for Robot Perception and Navigation.* Ph.D. thesis, Electrical and Computer Engineering Department, Carnegie-Mellon University.

Elfes, A. (1992). Dynamic Control of Robot Perception Using Multi-Property Inference Grids. *In: Proceedings of the 1992 IEEE International Conference on Robotics and Automation.* IEEE Press.

Engelson, S. (1994). *Passive Map Learning and Visual Place Recognition.* Ph.D. thesis, Yale University, Department of Computer Science.

Etienne, A. (1985). The Control of Short-Distance Homing in the Golden Hamster. *Pages 233–251 of:* Ellen, P., & Thinus-Blanc, C. (eds), *Cognitive Processes and Spatial Orientation in Animals and Man.* Boston, MA: Martinus Nijhoff.

Etienne, A. (1992). Navigation of a Small Mammal by Dead Reckoning and Local Cues. *Current Directions in Psychological Science*, **1**(2), 48–52.

Etienne, A., Teroni, V., Hurni, C., & Portenier, V. (1990). The Effect of A Single Light Cue on Homing Behaviour of the Golden Hamster. *Animal Behavior*, **39**, 17–41.

Etienne, A., Maurer, R., & Seguinot, V. (1996). Path Integration in Mammals and its Interaction with Visual Landmarks. *The Journal of Experimental Biology*, **199**(1), 201–209.

Everett, H. (1995). *Sensors for Mobile Robots: Theory and Application.* Wellesley, MA: A. K. Peters Ltd.

Foster, T., Castro, C., & McNaughton, B. (1989). Spatial Selectivity of Rat Hippocampal Neurons: Dependence on Preparedness for movement. *Science*, **244**, 1580–1582.

Gallistel, C. (1990). *The Organization of Learning.* Cambridge, MA: Bradford-MIT Press.

Gallistel, C., & Cramer, A. (1996). Computations on Metric Maps in Mammals: Getting Oriented and Choosing a Multi-Destination Route. *The Journal of Experimental Biology*, **199**(1), 211–217.

Gelb, A. (1974). *Applied Optimal Estimation.* MIT Press.

Hebb, D. (1949). *The Organization of Behavior.* New York: John Wiley & Sons.

Hebert, P., Betge-Brezetz, S., & Chatila, R. (1995). Probabilistic Map Learning: Necessity and Difficulties. *Pages 307–321 of: Proceedings of the International Workshop on Reasoning with Uncertainty in Robotics.* Springer-Verlag.

Hull, C. (1934a). The Concept of Habit-Family Hierarchy and Maze Learning. I. *Psychological Review*, **41**, 33–54.

Hull, C. (1934b). The Concept of Habit-Family Hierarchy and Maze Learning. II. *Psychological Review*, **41**, 134–152.

Hwang, Y., & Ahuja, N. (1992). Gross Motion Planning – A Survey. *ACM Computing Surveys*, **24**(3), 219–291.

Jazwinski, A. (1970). *Stochastic Processes and Filtering Theory.* New York, NY: Academic Press.

Jensen, O., & Lisman, J. (1996). Hippocampal CA3 Region Predicts Memory Sequences: Accounting for the Phase Precession of Place Cells. *Learning and Memory*, **3**, 279–287.

Johnson, R., & Bhattacharyya, G. (1996). *Statistics: Principles and Methods.* John Wiley and Sons.

Jung, M., & McNaughton, B. (1993). Spatial Selectivity of Unit Activity in the Hippocampal Granular Layer. *Hippocampus*, **3**, 165–182.

Kalman, R. (1960). A New Approach to Linear Filtering and Prediction Problems. *Transactions of the ASME*, **60**.

Kaplan, S. (1973a). Cognitive Maps, Human Needs, and the Designed Environment. *In:* Preiser, W. (ed), *Environmental Design Research, Vol 1.* Dowden, Hutchinson, and Ross.

Kaplan, S. (1973b). Cognitive Maps in Perception and Thought. *In:* Downs, M., & Stea, D. (eds), *Image and Environment.* Aldine Publishing Company.

Keith, J., & McVety, K. (1988). Latent Place Learning in a Novel Environment and the Influences of Prior Training in Rats. *Psychobiology*, **16**(2), 146–151.

Knierim, J., Kudrimoti, H., & McNaughton, B. (1995). Hippocampal Place Fields, the Internal Compass, and the Learning of Landmark Stability. *Journal of Neuroscience*, **15**, 1648–1659.

Kortenkamp, D. (1993). *Cognitive Maps for Mobile Robots: A Representation for Mapping and Navigation.* Ph.D. thesis, University of Michigan, Electrical Engineering and Computer Science Department.

Kortenkamp, D., & Weymouth, T. (1994). Topological Mapping for Mobile Robots Using a Combination of Sonar and Vision Sensing. *In: AAAI-94: Proceedings of the Americal Association of Artificial Intelligence.*

Kubie, J., & Ranck, J. (1983). Sensory-Behavioral Correlates in Individual Hippocampus Neurons in Three Situations: Space and Context. *Pages 433–447 of:* Seifert, W. (ed), *Neurobiology of the Hippocampus.* London: Academic Press.

Kuipers, B. (1978). Modeling Spatial Knowledge. *Cognitive Science*, **2**, 129–153.

Kuipers, B., & Byun, Y-T. (1991). A Robot Exploration and Mapping Strategy Based on a Semantic Hierarchy of Spatial Representations. *Robotics and Autonomous Systems*, **8**.

Kuipers, B., Froom, R., Lee, W., & Pierce, D. (1993). The Semantic Hierarchy in Robot Learning. *Chap. 6, pages 141–170 of:* Connell, J., & Mahadevan, S. (eds), *Robot Learning.* MA: Kluwer Academic Publishers.

Langley, P., & Pfleger, K. (1995). Acquisition of Place Knowledge Through Case-Based Learning. *In: Proceedings of the International Conference on Machine Learning.*

Latombe, J-C. (1991). *Robot Motion Planning.* Kluwer Academic.

Leonard, J., & Durrant-Whyte, H. (1992). Dynamic Map Building for and Autonomous Mobile Robot. *International Journal of Robotics Research*, **11**(4).

Levitt, T., & Lawton, D. (1990). Qualitative Navigation for Mobile Robots. *Artificial Intelligence*, **44**(3), 305–360.

Levy, W. (1989). A Computational Approach to Hippocampal Function. *The Psychology of Learning and Motivation*, **23**, 243–305.

Marr, D. (1971). Simple Memory: A Theory for Archicortex. *Philosophical Transactions of the Royal Society of London*, **176**, 23–81.

Mataric, M. (1992). Integration of Representation into Goal-Driven Behavior-Based Robots. *IEEE Transactions on Robotics and Automation*, **8**(3).

Maybeck, P. (1990). The Kalman Filter: An Introduction to Concepts. *In:* Cox, I.J., & Wilfong, G. T. (eds), *Autonomous Robot Vehicle*. Springer Verlag.

McNaughton, B. (1989). Neuronal Mechanisms for Spatial Computation and Information Storage. *Pages 285–350 of:* Nadel, L., Cooper, A., Culicover, P., & Harnish, R. (eds), *Neural Connections, Mental Computation*. Cambridge, MA: MIT Press.

McNaughton, B., & Nadel, L. (1989). Hebb-Marr Networks and the Neurobiological Representation of Action in Space. *Pages 1–63 of:* Gluck, M., & Rumelhart, D. (eds), *Neuroscience and Connectionist Theory*. Hillsdale, NJ: Lawrence Earlbaum Associates.

McNaughton, B., & Nadel, L. (1990). Hebb-Marr Networks and the Neurobiological Representation of Action in Space. *Pages 1–63 of:* Gluck, M., & Rumelhart, D. (eds), *Neuroscience and Connectionist Theory*. Hillsdale, NJ: Lawrence Earlbaum Associates.

McNaughton, B., Leonard, B., & Chen, L. (1989). Cortical-hippocampal Interactions and Cognitive Mapping: A Hypothesis Based on Reintegration of the Parietal and Inferotemporal Pathways for Visual Processing. *Psychobiology*, **17**(3), 230–235.

McNaughton, B., Knierim, J., & Wilson, M. (1995). Vector Encoding and the Vestibular Foundations of Spatial Cognition: A Neurophysiological and Computational Hypothesis. *Chap. 37 of:* Gazzaniga, M. (ed), *The Cognitive Neurosciences*. Boston:MIT Press.

McNaughton, B., Barnes, C., Gerrard, J., Gothard, K., Jung, M., Knierim, J., Kudrimoti, H., Qin, Y., Skaggs, W., Suster, M., & Weaver, K. (1996). Deciphering the Hippocampal Polyglot: the Hippocampus as a Path-Integration System. *The Journal of Experimental Biology*, **199**(1), 173–185.

Minai, A., & Levy, W. (1993). The Dynamics of Sparse Random Networks. *Biological Cybernetics*, **70**, 177–187.

Mittelstaedt, H., & Mittelstaedt, M. (1982). Homing by Path Integration in a Mammal. *Pages 290–297 of:* Papi, F., & Wallraff, H. (eds), *Avian Navigation*, vol. 67. Berlin: Springer-Verlag.

Mittelstaedt, M., & Mittelstaedt, H. (1980). Homing by Path Integration in a Mammal. *Naturwissenschaften*, **67**, 566–567.

Mizumori, S., & Williams, J. (1993). Directionally Selective Mnemonic Properties of Neurons in the Lateral Dorsal Nucleus of the Thalamus of Rats. *Journal of Neuroscience*, **13**, 4015–4028.

Moravec, H., & Elfes, A. (1985). High Resolution Maps from Wide Angle Sonar. *Pages 116–121 of: Proceedings of the 1985 IEEE International Conference on Robotics and Automation.*

Morris, R. (1981). Spatial Localization Does Not Require the Presence of Local Cues. *Learning and Motivation*, **12**, 239–261.

Morris, R., Garrud, P., Rawlins, J., & O'Keefe, J. (1982). Place Navigation Impaired in Rats with Hippocampal Lesions. *Nature*, **297**, 681–683.

Moutarlier, P., & Chatila, R. (1989). Stochastic Multisensory Data Fusion for Mobile Robot Location and Environment Modeling. *In: The Fifth International Symposium on Robotics Research.*

Muller, R., & Kubie, J. (1987). The Effects of Changes in the Environment on the Spatial Firing of Hippocampal Complex-Spike Cells. *Journal of Neuroscience*, **7**, 1951–1968.

Muller, R., Kubie, J., & Ranck, J. (1987). Spatial Firing Patterns of Hippocampus Complex-Spike Cells in a Fixed Environment. *Journal of Neuroscience*, **7**, 1935–1950.

Muller, R., Kubie, J., & Saypoff, R. (1991). The Hippocampus as a Cognitive Graph. *Hippocampus*, **1**(3), 243–246.

Nehmzow, U. (1995). Animal and Robot Navigation. *Robotics and Autonomous Systems*, **15**, 71–81.

O'Keefe, J. (1976). Place Units in the Hippocampus of the Freely Moving Rat. *Experimental Neurology*, **51**, 78–109.

O'Keefe, J. (1989). Computations the Hippocampus Might Perform. *Pages 225–284 of:* Nadel, L., Cooper, L., Culicover, P., & Harnish, R. (eds), *Neural Connections, Mental Computation.* Cambridge, MA: MIT Press/Bradford Book.

O'Keefe, J., & Dostrovsky, J. (1971). The Hippocampus as a Spatial Map: Preliminary Evidence from Unit Activity in the Freely Moving Rat. *Brain Research*, **34**, 171–175.

O'Keefe, J., & Nadel, L. (1978). *The Hippocampus as a Cognitive Map.* Oxford:Clarendon Press.

O'Keefe, J., & Speakman, A. (1987). Single Unit Activity in the Rat Hippocampus During a Spatial Memory Task. *Experimental Brain Research*, **68**, 1–27.

Potegal, M. (1972). The caudatenucleus egocentric localization system. *Acta Neurobiological Experiments*, **32**, 479–494.

Prepscius, C., & Levy, W. (1994). Sequence Prediction and Cognitive Mapping by a Biologically Plausible Neural Network. *Pages 164–169 of: Proceedings of the World Congress on Neural Networks.*

Prescott, T. (1995). Spatial Representations for Navigation in Animats. *Adaptive Behavior*, **4**(2), 85–123.

Prescott, T., & Mayhew, J. (1992). Building Long-Range Cognitive Maps Using Local Landmarks. *Pages 233–242 of:* Meyer, J., Roitblat, H., & Wilson, S. (eds), *Proceedings of the Second International Conference on Simulation of Adaptive Behavior.* Cambridge, MA: MIT Press, Bradford Book.

Quirk, G., Muller, R., & Kubie, J. (1990). The Firing of Hippocampal Place Cells in the Dark Depends on the Rat's Recent Experience. *Journal of Neuroscience*, **10**, 2008–2017.

Quirk, G., Muller, R., Kubie, J., & Ranck, J. (1992). The Positional Firing Properties of Medial Entorhinal Neurons: Description and Comparison with Hippocampal Place Cells. *Journal of Neuroscience*, **12**(5), 1945–1963.

Ranck, J. (1984). Head Direction Cells in the Deep Cell Layer of Dorsal Presubiculum in Freely Moving Rats. *Society for Neuroscience Abstracts*, **10**, 599.

Recce, M., & Harris, K. (1996). Memory for Places: A Navigational Model in Support of Marr's Theory of Hippocampal Function. *Hippocampus*, **6**, 735–748.

Redish, D., & Touretzky, D. (1996). Navigating with Landmarks: Computing Goal Locations from Place Codes. *In:* Ikeuchi, K., & Veloso, M. (eds), *Symbolic Visual Learning.* Oxford University Press.

Rolls, E. (1990). Functions of the Primate Hippocampus in Spatial Processing and Memory. *Pages 339–362 of:* Kesner, R., & Olton, D. (eds), *Neurobiology of Comparative Cognition.* Hillsdale, NJ: Lawrence Earlbaum Associates.

Rolls, E. (1996). The Representation of Space in the Primate Hippocampus and Episodic Memory. *Pages 375–400 of:* Ono, T., McNaughton, B., Molotchnikoff, S., Rolls, E., & Nishijo, H. (eds), *Perception, Memory, and Emotion: Frontiers in Neuroscience.* Pergamon.

Schmajuk, N. (1986). *Real-Time Attentional Models for Classical Conditioning and the Hippocampus.* Ph.D. thesis, University of Massachusetts, Amherst, MA.

Schmajuk, N., & Blair, H. (1993). Place Learning and the Dynamics of Spatial Navigation: A Neural Network Approach. *Adaptive Behavior*, **1**, 355–387.

Schmajuk, N., & DiCarlo, J. (1991). Neural Dynamics and Hippocampal Modulation of Classical Conditioning. *In:* Commons, M., Grossberg, S., & Staddon, J. (eds), *Neural Network Models of Conditioning and Action.* Lawrence Erlbaum Associates.

Schmajuk, N., & Thieme, A. (1992). Purposive Behavior and Cognitive Mapping: A Neural Network Model. *Biological Cybernetics*, **67**, 165–174.

Scholkopf, B., & Mallot, H. (1995). View-Based Cognitive Mapping and Path Planning. *Adaptive Behavior*, **3**(3), 311–348.

Schone, H. (1984). *Spatial Orientation: The Spatial Control of Behavior in Animals and Man.* Princeton, NJ: Princeton University Press.

Seibert, M., & Waxman, A. (1992). Adaptive 3D Object Recognition from Multiple Views. *IEEE Transactions on Pattern Analysis and Machine Intelligence*, **14**, 107–124.

Sharp, P. (1996). Multiple Spatial/Behavioral Correlates for Cells in the Rat Postsubiculum: Multiple Regression Analysis and Comparison to Other Hippocampal Areas. *Cerebral Cortex*, **6**, 238–259.

Sharp, P., & Green, C. (1994). Spatial Correlates of Firing Patterns of Single Cells in the Subiculum of the Freely Moving Rat. *Journal of Neuroscience*, **14**, 2339–2356.

Sharp, P., Kubie, J., & Muller, R. (1990). Firing Properties of Hippocampal Neurons in a Visually Symmetrical Environment: Contributions of Multiple Sensory Cues and Mnemonic Properties. *Journal of Neuroscience*, **10**, 2339–2356.

Skaggs, W., & McNaughton, B. (1996). Replay of Neuronal Firing Sequence in Rat Hippocampus During Sleep Following Spatial Experience. *Science*, **271**, 1870–1873.

Smith, R., Self, M., & Cheeseman, P. (1990). Estimating Uncertain Spatial Relationships in Robotics. *In:* Cox, I., & Wilfong, G. (eds), *Autonomous Robot Vehicles*. Springer-Verlag.

Squire, L., Shimamura, A., & Amaral, D. (1989). Memory and the Hippocampus. *Pages 208–239 of:* Byrne, J., & Berry, W. (eds), *Neural Models of Plasticity: Theoretical and Empirical Approaches*. New York, NY: Academic Press.

Sutherland, R., Whishaw, I., & Kolb, B. (1982). A Behavioural Analysis of Spatial Localization Following Electrolytic, Kainate- or Colchicine-Induced Damage to the Hippocampal Formation in the Rat. *Behavioural Brain Research*, **7**, 133–153.

Taube, J. (1995). Head-Direction Cells Recorded in the Anterior Thalamic Nuclei of Freely Moving Rats. *Journal of Neuroscience*, **15**, 70–86.

Taube, J., Muller, R., & Ranck, J. (1990a). Head Direction Cells Recorded from the Postsubiculum in Freely Moving Rats: I. Description and Quantitative Analysis. *Journal of Neuroscience*, **10**, 420–435.

Taube, J., Muller, R., & Ranck, J. (1990b). Head Direction Cells Recorded from the Postsubiculum in Freely Moving Rats: II. Effects of Environmental Manipulations. *Journal of Neuroscience*, **10**, 436–447.

Thrun, S. (1996). *A Bayesian Approach to Landmark Discovery and Active Perception in Mobile Robot Navigation*. Tech. rept. CMU-CS-96-122. Carnegie Mellon University, Pittsburgh, USA.

Tolman, E. (1948). Cognitive Maps in Rats and Men. *Psychological Review*, **55**, 189–208.

Traub, R., & Miles, R. (1991). *Neuronal Networks of the Hippocampus*. Cambridge University Press.

Trullier, O., Wiener, S., Berthoz, A., & Meyer, J-A. (1997). Biologically-based Artificial Navigation Systems: Review and Prospects. *Progress in Neurobiology*, **51**, 483–544.

Tsuji, S., & Li, S. (1993). Memorizing and Representing Route Scenes. *In: Proceedings of the Second International Conference on Simulation of Adaptive Behavior*. MIT Press.

Wan, H., Touretzky, D., & Redish, A. (1994). Towards a Computational Theory of Rat Navigation. *Pages 11–19 of:* Mozer, M., Smolensky, P., Touretzky, D., Elman, J., & Weigend, A. (eds), *Proceedings of the 1993 Connectionist Models Summer School.* Lawrence Earlbaum Associates.

Wehner, R. (1992). Homing in Arthropods. *Pages 45–144 of:* Papi, F. (ed), *Animal Homing.* London: Chapman & Hall.

Wehner, R., & Srinivasan, M. (1981). Searching Behavior of Desert Ants, Genus Cataglyphis (Formicidae, Hymenoptera). *Journal of Comparative Physiology*, **142**, 315–338.

Wilson, M., & McNaughton, B. (1993). Dynamics of the Hippocampal Ensemble Code for Space. *Science*, **261**, 1055–1058.

Worden, R. (1992). Navigation by Fragment Fitting: A Theory of Hippocampal Function. *Hippocampus*, **2**(2), 165–188.

Yamauchi, B., & Beer, R. (1996). Spatial Learning for Navigation in Dynamic Environments. *IEEE Transactions on Systems, Man, and Cybernetics - Part B, Special Issue on Robot Learning*, **26**.

Yamauchi, B., & Langley, P. (1997). Place recognition in Dynamic Environments. *Journal of Robotic Systems, Special Issue on Mobile Robots*, **14**(2), 107–120.

Zipser, D. (1986). Biologically Plausible Models of Place Recognition and Place Location. *Pages 432–470 of:* Rumelhart, D., McClelland, J., & the PDP Research Group (eds), *Parallel Distributed Processing: Explorations in the Micro-Structure of Cognition, Volume 2.* Cambridge, MA: MIT Press.

Appendix

Proposition 1 (Size of the EC fields) *In two dimensional space the EC field, or the region over which it responds, is roughly* circular *with a radius of* $r \leq \sqrt{-2\sigma_L^2 \ln(, _{EC})}$.

If the variance of the EC cell distance matching Gaussians is given by σ_L^2 and the EC cell is said to recognize a landmark if the cell activation is greater than the threshold of $, _{EC}$, then the range over which the EC cell with center (c_x, c_y) responds is given by:

$$\exp^{-\frac{(x-c_x)^2+(y-c_y)^2}{2\sigma_L^2}} \geq , _{EC} \Longleftrightarrow (x-c_x)^2 + (y-c_y)^2 \leq -2\sigma_L^2 \ln(, _{EC}) \Longleftrightarrow r^2 \leq -2\sigma_L^2 \ln(, _{EC}) \quad (12)$$

Thus, with $\sigma_L^2 = 2.25$ and $, _{EC} = 0.6$, we obtain $r \leq 1.51$, i.e., the EC unit responds to a landmark within a circular region of radius 1.5 from its center.

Proposition 2 (Variance of an EC cell) *The variance associated with an EC unit is given by* $\sigma = \sqrt{R^2\sigma_S^2 - 2\sigma_L^2 \ln , _{EC}}$

The variance associated with an EC unit firing has two components. The first component is a measure of the uncertainty associated with the EC unit center, while the second component is the imprecision tolerated by the EC firing field. Suppose the sensory range error is characterized by a zero-mean, white Gaussian with standard deviation σ_S (per unit distance), and the maximum sensory range is R. When a new EC unit is recruited and its center is set up, the imprecision (or uncertainty) associated with the center is characterized by the sensing uncertainty and has a variance of $R^2\sigma_S^2$. From proposition 1, the position uncertainty within the EC field is given by $r^2 \leq -2\sigma_L^2 \ln(, _{EC})$. Since these two sources of uncertainty are independent, the net variance associated with an EC cell is given by: $\sigma^2 = R^2\sigma_S^2 - 2\sigma_L^2 \ln , _{EC}$.

Proposition 3 (Measurement error has a specific form) *The measurement error is given by* $w_k = x_{i_k} - x_{0,k}$.

In our model the measurement function is assumed to represent the distance between the current position of the animal and the center of the place field that it is currently in, i_k, corrupted by some random measurement noise. Thus

$$z_k = x_{0,k} - x_{i_k} + w_k$$

Since the true centers of the place fields are not known, and the true position of the animal is unknown (and is the very subject of this localization process), z_k cannot be measured. In our model we assume that the animal always measures 0, which constrains the form of the random noise to:

$$z_k = x_{0,k} - x_{i_k} + w_k = 0 \implies w_k = x_{i_k} - x_{0,k} \tag{13}$$

Thus, Kalman filtering in our model uses observed measurement of 0 and predicted measurement of $\hat{x}_{0,k} - \hat{x}_{i_k}$ to perform the required updates.

Proposition 4 (Measurement error has zero mean) $E(w_k) = 0$

In order to use Kalman filtering, we have to show that our measurement noise has zero mean. As shown in proposition 3, the measurement noise is given by $w_k = x_{i_k} - x_{0,k}$. Thus:

$$E(w_k) = \int \sum_{\text{places } p} (x_p - x_{0,k}) \Pr(x_{0,k}/p) \Pr(p/k) dx_{0,k}$$

$$\iff E(w_k) = \sum_{\text{places } p} \underbrace{\int (x_p - x_{0,k}) \Pr(x_{0,k}/p) dx_{0,k}}_{0} \Pr(p/k) \iff E(w_k) = 0$$

Notice that the noise is zero-mean only if there is no prior bias on the position of the animal in the place field, i.e., each position in the place field is either equiprobable or when the animal is assumed to navigate from one place field *center* to another.

Proposition 5 (Measurement error is autocorrelated) *The measurement error w_k is autocorrelated, i.e., $E(w_k w_{k-1}^T) \neq 0$.*

At time step $k-1$, suppose the robot was at the position $x_{0,k-1}$. Suppose the sensor inputs determined that the robot was in place i_{k-1} with place field center $x_{i_{k-1}}$. Then:

$$w_{k-1} = x_{i_{k-1}} - x_{0,k-1} \tag{14}$$

Since the robot moves by u_{k-1} (and assuming linear robot transformations), its position at step k is given by:

$$x_{0,k} = x_{0,k-1} + u_{k-1} \tag{15}$$

Suppose this position corresponds to place i_k with center x_{i_k}, then:

$$w_k = x_{i_k} - x_{0,k} \tag{16}$$

Using equations 15 and 14 in 16, we get:

$$w_k = x_{i_k} - x_{i_{k-1}} - u_{k-1} + w_{k-1} \tag{17}$$

As can be observed, w_k depends on w_{k-1}, and hence is an autocorrelated sequence.

Proposition 6 (Covariance in the Mahalanobis test) *The covariance matrix of the Mahalanobis distance test used in section 8.5 is given by $(C_{ii} + C_{00} - 2C_{0i} + \mathbf{R}_k)$*

Suppose we are considering CA1 unit i with true place field center x_i and estimated center $\hat{x}_i$. Since predictions in our model are given by $\hat{z}_k = \hat{x}_{0,k} - \hat{x}_i$ while the observations are given by $z_k = x_{0,k} - x_i + w_k$, we can determine the covariance between the predicted and observed measurements of the Mahalanobis test for CA1 unit i.

$$E((\hat{z}_k - z_k)(\hat{z}_k - z_k)^T) \tag{18}$$

$$\iff E((\hat{x}_{0,k} - \hat{x}_i - x_{0,k} + x_i - w_k)(\hat{x}_{0,k} - \hat{x}_i - x_{0,k} + x_i - w_k)^T) \tag{19}$$

$$\iff E((\epsilon_i - \epsilon_{0,k} - w_k)(\epsilon_i - \epsilon_{0,k} - w_k)^T) \tag{20}$$

$$\iff C_{ii} + C_{00} - 2C_{0i} + \mathbf{R}_k \tag{21}$$

Note that we assume that the dead-reckoning and measurement noises are independent, i.e. $E(\epsilon_i w_k^T) = E(\epsilon_{0,k} w_k^T) = E(w_k \epsilon_i^T) = E(w_k \epsilon_{0,k}^T) = 0$.

Proposition 7 (Chi-square (χ^2) distribution and the Mahalanobis test) *The distance threshold for the Mahalanobis test is 4.61*

The probability density function of a χ^2 distribution is an asymmetric curve with a long right-hand tail. Given the number of degrees of freedom, we can determine the value of the distribution (χ^2_α) such that the area under the curve to the right of it α (Johnson & Bhattacharyya, 1996). Since the Mahalanobis distance has a chi-square distribution, we can choose a value of the distance such that the area to the right of it is, say, 10%. Since the covariance matrix of the Mahalanobis test shown in proposition 6 has a rank of 2, we determine the value of the chi-square distribution with 2 degrees of freedom, such that the area to the right of it is 10%. This value is 4.61 (Johnson & Bhattacharyya, 1996).

Thus, in our model, if we compute the Mahalanobis distance and declare that the match is correct if this distance happens to be less than 4.61, then we can be 90% confident of *not* rejecting actually correct matches.

Proposition 8 (The 2.5σ boundary) *The 2.5σ boundary around an estimated parameter is expected to include the true value with probability greater than 84%*

According to Chebyshev's inequality, if μ and σ are the mean and standard deviation of a random variable X, then for any positive constant k:

$$\Pr(|X - \mu| < k\sigma) \geq 1 - \frac{1}{k^2} \tag{22}$$

Thus, if x_i is the estimated parameter with current estimate $\hat{x}_i$ and variance σ, using $k = 2.5$ in Chebyshev's theorem yields:

$$\Pr(|x_i - \hat{x}_i| < 2.5\sigma) \geq 0.84 \tag{23}$$

Thus, the 2.5σ boundary is expected to include the true value with probability greater than 84%.